Analytical Methods for Power Monitoring and Control in an Underwater Observatory

Ting Chan

A dissertation submitted in partial fulfillment of the
requirements for the degree of

Doctor of Philosophy

University of Washington

2007

Program Authorized to Offer Degree: Electrical Engineering

University of Washington
Graduate School

This is to certify that I have examined this copy of a doctoral dissertation by

Ting Chan

and have found that it is complete and satisfactory in all respects,
and that any and all revisions required by the final
examining committee have been made.

Chair of the Supervisory Committee:

_____
Chen-Ching Liu

Reading Committee:

_____
Chen-Ching Liu

_____
Mark Damborg

_____
Bruce Howe

Date: _____

In presenting this dissertation in partial fulfillment of the requirements for the doctoral degree at the University of Washington, I agree that the Library shall make its copies freely available for inspection. I further agree that extensive copying of the dissertation is allowable only for scholarly purposes, consistent with "fair use" as prescribed in the U.S. Copyright Law. Requests for copying or reproduction of this dissertation may be referred to Proquest Information and Learning, 300 North Zeeb Road, Ann Arbor, MI 48106-1346, 1-800-521-0600, to whom the author has granted "the right to reproduce and sell (a) copies of the manuscript in microform and/or (b) printed copies of the manuscript made from microform."

Signature_____

Date_____

University of Washington

Abstract

Analytical Methods for Power Monitoring and Control in an Underwater Observatory

Ting Chan

Chair of the Supervisory Committee:
Professor Chen-Ching Liu
Department of Electrical Engineering

The study of the undersea environment requires the use of scientific instruments at the bottom of the ocean and in the water column to collect useful data. The traditional methods of conducting such studies by sending ships or using bottom instruments and moorings are not able to provide the necessary data over a long period of time due to weather and energy limitations. The objective of the North Eastern Pacific Time-Series Undersea Networked Experiment (NEPTUNE) program is to construct an underwater cabled observatory on the seafloor of the northeast Pacific Ocean off the coast of Washington, Oregon, and British Columbia, encompassing the Juan de Fuca Tectonic Plate. This system features over a few dozens of science nodes for the connection of scientific instruments that enhance our ability to conduct continuous ocean studies in this region. This dissertation investigates important design and implementation issues of the NEPTUNE power system.

The power system associated with the proposed observatory is unlike conventional terrestrial power systems in many ways due to the unique operating conditions of underwater cabled observatories including the high reliability requirements and low observability and controllability. These unique aspects of the NEPTUNE system lead to the development of new hardware and software

applications that will provide an essential and efficient operation environment. In this dissertation, the solutions to some of the technical problems are proposed.

The design of the Power Monitoring and Control System (PMACS) allows PMACS to function in a similar way that Supervisory Control and Data Acquisition (SCADA) and Energy Management Systems (EMS) are used to monitor and control terrestrial systems. A Fault Location algorithm is developed to identify a backbone cable fault by solving nonlinear equations with only shore station measurements. The same approach can be applied to underground power systems. In order to handle the request from the science users to turn their loads on and off, a Load Management algorithm is proposed based on nonlinear optimization. This algorithm takes into account the different priorities of science node loads. The PMACS EMS modules require different parameters in the system model to provide accurate results. The effect of cable resistance variation due to the temperature of the seawater is investigated and an algorithm is developed for PMACS to update the resistance values using a quadratic programming technique.

The algorithms developed in this research addresses challenges and difficulties for an underwater observatory system. The results presented in this dissertation should be applicable to similar underwater systems in the future.

Table of Contents

Page

List of Figures

Figure Number Page

List of Tables

Table Number Page

Acknowledgements

I would like to express my sincere gratitude to my advisor, Professor Chen-Ching Liu, for his guidance, patience, support and inspiration throughout my studies in pursuing my PhD. During my study, he has provided me valuable suggestions with his expertise on various technical problems. I was given a high degree of freedom to explore the problems and solutions. His encouragements and suggestions have helped me to understand new perspective on the problems I have faced. I would also like to thank Dr. Bruce Howe, Professor Mark Damborg, and Professor Steve Shen for their guidance as members of the supervisory committee.

I would like the thank the engineers in the NEPTUNE power group, Dr. Harold Kirkham, Dr. Bruce Howe, Professor Mohammad El-Sharkawi, Tim McGinnis, Chris Siani and others. Working with them has been a good experience for me which showed me how a large project can be conducted with good teamwork and organization. The work on the NEPTUNE power system was funded by the National Science Foundation grant OCE 116750, "Development of a Power System for Cabled Ocean Observatories".

Special acknowledgement and thanks go to the members of the Applied Physics Laboratory for the development of PMACS, Tim McGinnis and Chris Siani for their work on the PMACS hardware, Mike Kenney for his work on the PMACS Server and NPC software, and John Elliott for his suggestions on PMACS Console design and implementation.

During the time I pursued my research, I received a lot of supports and assistance from the fellow graduate students. My thanks go to Dr. Juhwan Jung, Dr. Sung Kwan Joo, Dr. Hao Li, Dr. Kevin Schneider, Dr. Guang Li, Mr. Andrew Hartono, and Mr. Chung-I Lin for their friendship.

I would also like to thank Philip Pilgrim, Phil Lancaster, Wayne Beckman, and Hongrui Liu for their valuable suggestions in this research.

Last but not least, I would like to thank my wife, Sara Shum, for her constant support, encouragement, and understanding throughout the entire process of this research. My deepest gratitude goes to my parents for their love and support.

DEDICATION

To

My Family

Chapter 1: Introduction

The study of the undersea environment requires the use of scientific instruments at the bottom of the ocean to collect useful data. The traditional method of conducting such studies is to send a ship to the location of interest to collect data. Due to the limitation of weather condition, space and time, the information that can be collected is very limited. Long-term ocean observatory systems need to be built so that continuous electrical power can be supplied to science users. This enables the scientific instruments to operate over a much longer period of time without interruption. There are currently two types of ocean observatory systems: moorings and cabled observatory.

The first type requires the placing of buoys and junction boxes on the surface and the bottom of the ocean. This instrumentation has typically used batteries or a generator placed inside the buoys for its electrical power requirements [1]. The data collected are transmitted back to shore via satellite telecommunications. The battery life and fuel capacity severely restricts the duration as well as the efficiency with which the studies are conducted.

The second type of ocean observatory is designed by connecting multiple science nodes at the bottom of the ocean by submarine telecommunication cables from the shore. Continuous power is supplied to the science nodes from the shore. The communication capability also enables the collection and transmission of real-time data. Three different ocean cabled observatories are being developed over the world: NEPTUNE in North America, ARENA in Japan [2], and ESONET in Europe [3]. The designs are fundamentally different from one another while aiming at different requirements and tradeoffs [4]. For example, earthquakes occur periodically in Japan since it is located near plate boundaries. As a result, one of the primary requirements of the ARENA power system design is the ability to continue system operation when there is a disturbance such as catastrophic earthquakes or shunt cable fault to monitor

the seismic activity. ARENE therefore adopted a constant current power feeding design which is robust against cable faults. On the other hand, the NEPTUNE power system is based on a constant voltage power feeding approach. This design allows the system to deliver a larger amount of power to the science nodes than the constant current approach. In this dissertation, several aspects of the NEPTUNE system are discussed in details.

1.1 Overview of NEPTUNE

The objective of the North Eastern Pacific Time-Series Undersea Networked Experiment (NEPTUNE) program is to construct an underwater cabled observatory on the floor of the Pacific Ocean, encompassing the Juan de Fuca Tectonic Plate. The underwater scientific instruments connected to the system can be operated for long-term sustained measurements with real-time two-way communication using the observatory's fiber-optic/power cable, facilitating a host of new experimental capabilities [5]-[9].

The deployment of NEPTUNE will provide a wide range of scientific data of oceanographic, geological, and ecological processes. Real-time and archived data collected by the instruments connected to the system at the bottom of the ocean and in the water column can be provided to scientists, engineers, educators, decision makers, and learners of all ages with the Internet [10]. The essential elements of the NEPTUNE system are shown in Figure 1.1.

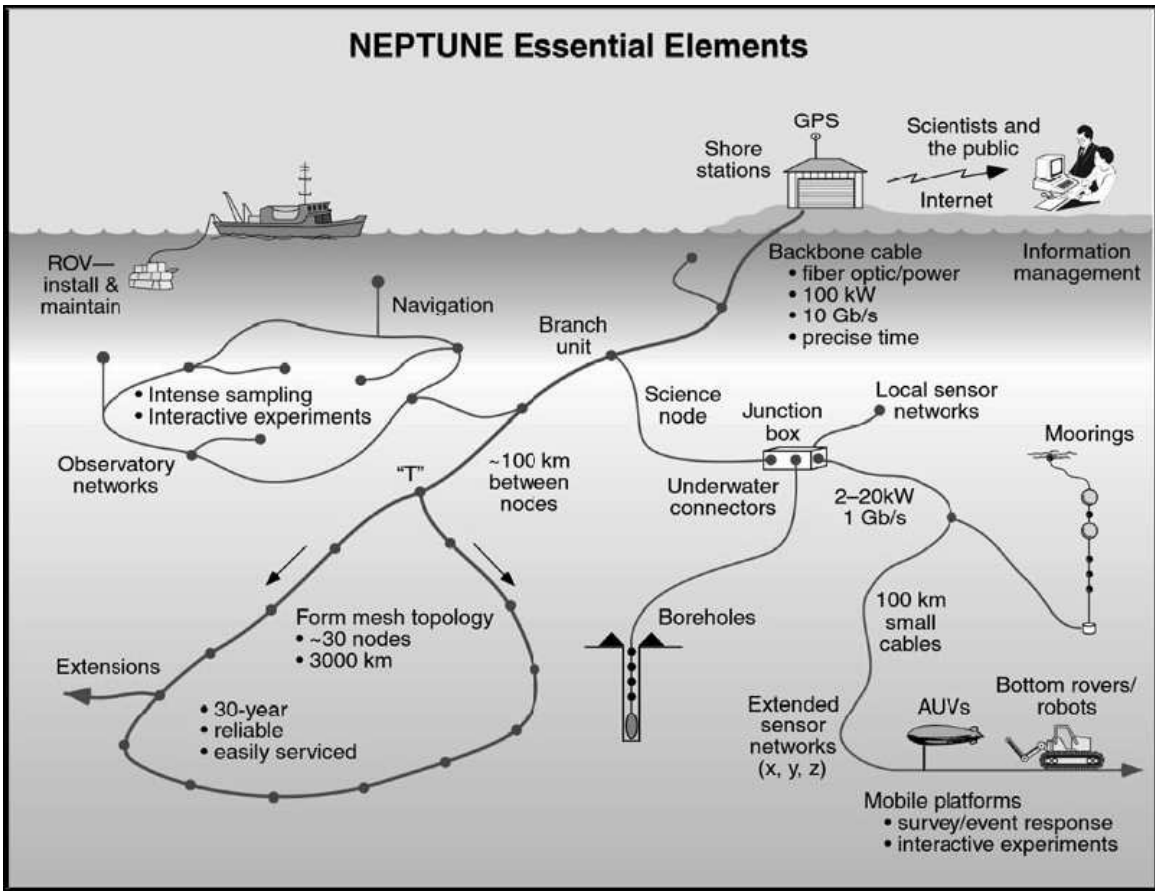

Figure 1.1: Essential elements of the NEPTUNE system

Traditional terrestrial power systems are normally AC networked parallel configurations while underwater telecommunication systems are normally DC series cabled systems. The proposed NEPTUNE power system differs from both of them in that the NEPTUNE power system is a DC networked system. It is planned to have approximately 3000 km of cables with 2 shore stations (Victoria and Nedonna Beach) and up to 46 science nodes, as illustrated in Figure 1.2. At each of the shore stations, a −10 kV DC power supply will be used to provide power that serves the entire system.

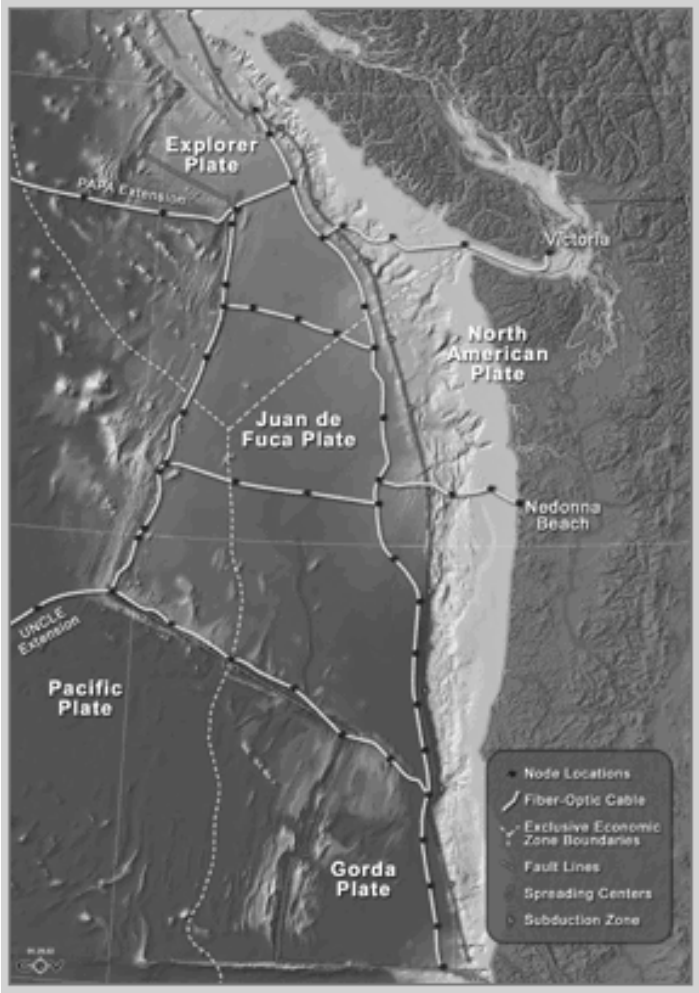

Figure 1.2: The NEPTUNE system

The cable connecting the science nodes is called the backbone. At each of the node locations, a branching unit (BU) is used to connect the backbone cable with the science node through a spur cable. The connection with the backbone cable, BU, and the science node is shown in Figure 1.3. In case of a backbone or spur cable fault, switches in the BU will be opened to isolate the fault so that the rest of the system will remain in operation. The power supply for the switches inside the BU is based on Zener diodes. The operation of a BU does not require explicit communications from the shore stations or science nodes [11]; several different voltage levels provide the

minimal necessary implicit communication. The design of the BU and the operation of the switches is presented in [12]. Voltages and currents on the backbone are not known to the operation center since no measuring device is installed. In the current design, the length of the backbone cable between each of the BUs ranges from tens of kilometers to over a hundred kilometers. The lengths of spur cables would be several to tens of kilometers.

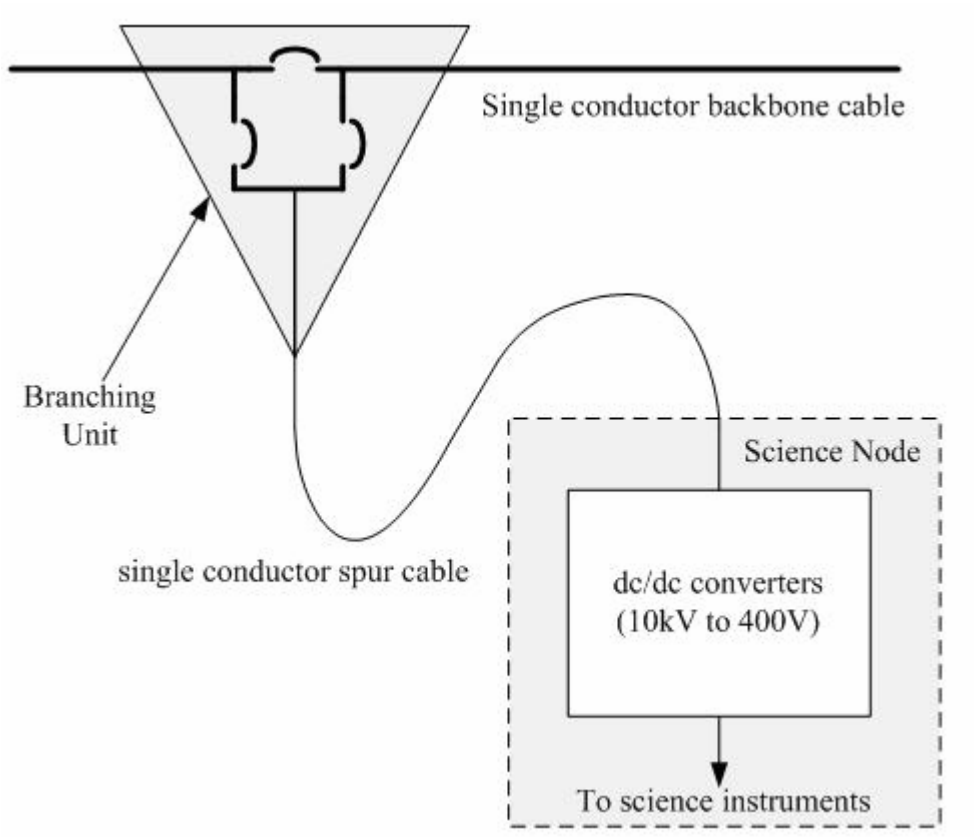

Figure 1.3: Connections between the backbone cable and science node

At each of the science nodes, a DC-DC power converter is used to convert the voltage level down to 400 V and 48 V for science users. The loads at the science nodes have a constant power characteristic due to the nature of the DC-DC converters. Changes in power levels do not have a significant impact on the loads.

The original proposed NEPTUNE system as shown in Figure 1.2 has been scaled back significantly. Figure 1.4 shows a recent configuration [13]. This new design has approximately 2000 km of backbone cables and about a dozen science nodes. The algorithms developed in this study are based on the original design and can be easily adapted to the new design.

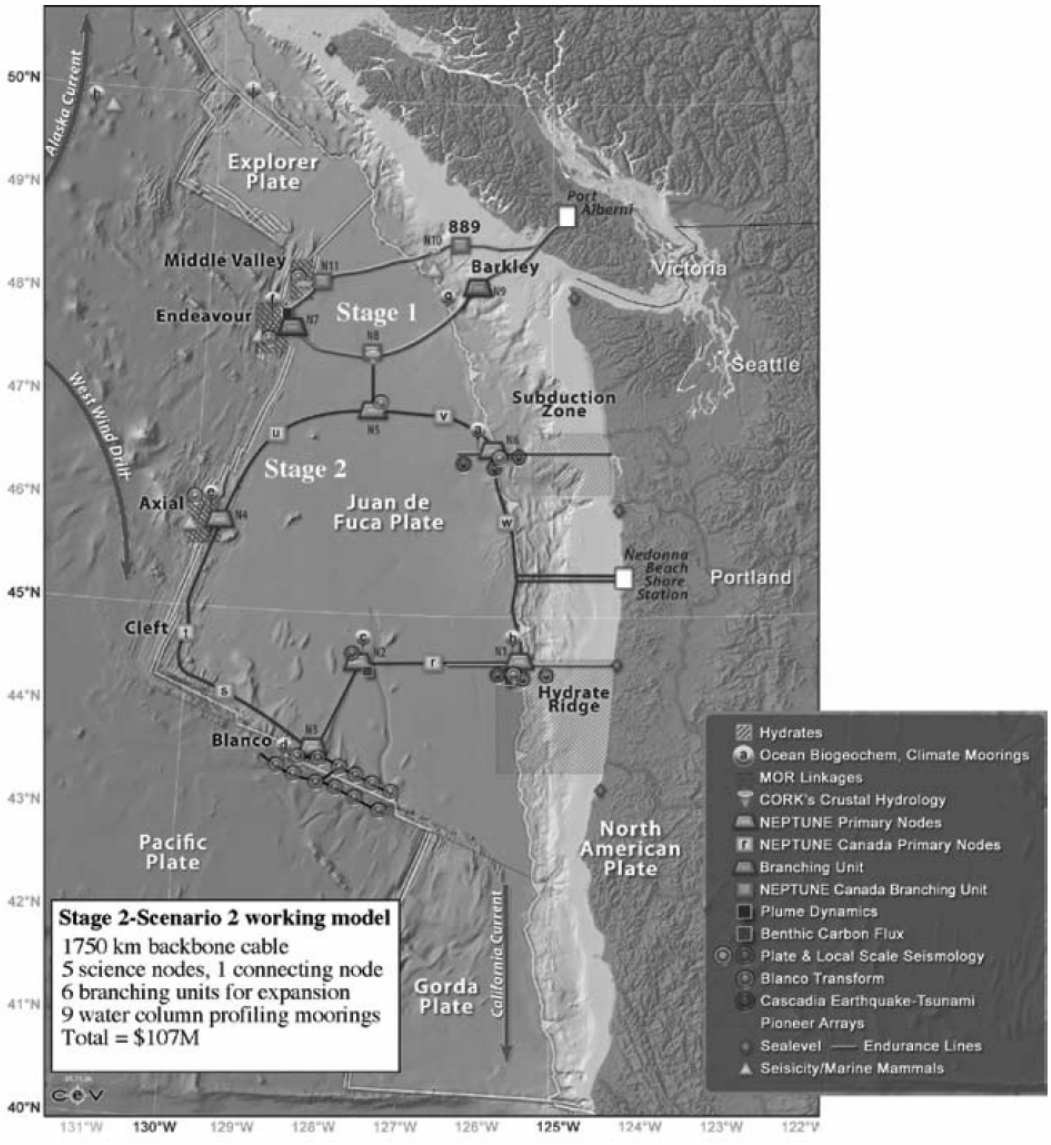

Figure 1.4: Recent design of NEPTUNE

Stage 1 of this new design is presently under construction by NEPTUNE Canada [14]. This regional cabled ocean observatory will be the northern portion of NEPTUNE. It will be a 4-node, 800 km loop terminated at Port Alberni. It will use a hybrid series-parallel power system. The series portion will power optical repeaters and the optical supervisory system that will, among other functions, control the BU breakers.

1.2 Contributions of this Dissertation

The design of the NEPTUNE power system involves a number of engineering challenges due to its physical location and the nature of a DC networked configuration: The repair/replacement cost of a component for an underwater observatory system can be very high. Therefore, a crucial design criterion for the NEPTUNE system is a very high level of reliability. The NEPTUNE system has to provide reliable power and communications to the science nodes for a life span of 30 years [7]. It is also our goal to design and implement the system so that minimum maintenance is required over the life span. The reliability requirement results in a system that uses simple designs for the system components which leads to the low observability of system status. This dissertation addresses a number of issues related to the design and implementation of an underwater observatory system by developing new monitoring and control technologies and computational methods.

1.2.1 Power Monitoring and Control System (PMACS)

The monitoring and control of a conventional terrestrial power system is handled by the Supervisory Control and Data Acquisition System (SCADA) system and Energy Management System (EMS) [15]-[17]. As an underwater observatory system,

the NEPTUNE power system needs to be able to monitor system parameters such as node voltages and switch status and perform control operations such as adjusting voltage outputs and switching of loads. Analytical methods for various system aspects need to be developed.

For NEPTUNE, a Power Monitoring and Control System (PMACS) is developed that combines the functionalities of SCADA and EMS. The purpose of PMACS is to provide computer, communication and software facilities for system operators to monitor and control the system. As a result, a number of modules for PMACS are developed to provide functions such as fault location, state estimation, load management and topology identification. The modules for state estimation and topology identification are developed by Schneider [18]. The modules for fault location and load management are presented in later chapters of this dissertation. The design and architecture of PMACS is discussed in Chapter 2.

1.2.2 Fault location

One of the main challenges of the NEPTUNE power system is to identify the location of a backbone cable fault. Since limited resources are available for the development of a communications system of adequate reliability, it was decided that no communication would be available from shore stations to the branching units. As a result, voltages and currents on the backbone and the status of BU switches are not known to the operation center at the shore stations. Unlike traditional power systems, the fundamental assumption is that no instantaneous fault data will be available since no recording devices and communications are available on the backbone cable.

In the design of NEPTUNE, a single backbone cable fault would not cause a loss of any science node in most locations after the fault is isolated. However, in case a section of the backbone cable is missing, the total power that can be delivered to science nodes can be affected depending on the fault location. Therefore, the faulted

cable has to be repaired in order to allow the system to operate at full load. In case of a backbone cable fault, a repair ship is sent to the estimated location of the fault. Deep sea repairs can be slow and costly; therefore, the Fault Location module of PMACS is intended to locate a backbone cable fault to within ±1 km.

Typical terrestrial power system techniques require the use of measuring devices such as Digital Fault Recorder and Phasor Measurement Unit [19]-[20]. The analysis is done by observing the operations of the circuit breakers and the transients of voltages. Due to the physical size of the branching units, measuring devices cannot be installed. The above techniques cannot be applied for lack of these devices. The use of Time Domain Reflectometry [21] for submarine cable fault location cannot be used in this system due to the networked configuration and the size of the system. The reflect signal is too small to be distinguished from noise since the fault might be located thousand of kilometers away from the source.

In this research, a fault location algorithm is developed based on the available measurements of voltage and current outputs from the shore stations during a backbone cable fault. The algorithm uses knowledge of the system topology and solves for the location of the fault with a set of nonlinear equations. While typical resistance estimation method for underwater application is done in a point-to-point manner, the algorithm developed in this study generalizes the procedure by expending the application to a networked system. The development and implementation of the fault location algorithm is presented in Chapter 3.

1.2.3 Load Management

Load management is used in conventional power systems to reduce the costs of operation and increase reliability margin [22]. The methods are normally based on optimization techniques by maximizing the profit or minimizing the cost. However,

for the NETPUNE system, the object of load management is to provide the maximum amount of power to the science node loads without violating any system constraints.

The total power that the NEPTUNE power system can supply to the science nodes is limited by the voltage outputs of the shore station power supplies and the current limit of the backbone cable. The nominal voltage output of the power supply at each shore station is 10kV. The backbone cables have a nominal 10A current limit. Therefore, the maximum total power the system can provide at any given time is 200kW. Each individual science node can consume up to 10kW. It is clear that the system would not be able to simultaneously supply the maximum load at every science node.

The loads at the science nodes are categorized into different priorities. Since power is a limited resource, it is to be reserved for loads with high priorities in the case when all loads can not be served. A method for deciding the appropriate action is needed. For this purpose, a Load Management module using non-linear optimization based techniques is developed to determine the maximum amount of power that the system can supply to the individual science nodes without violating any of the system constraints. This algorithm takes into account the load priorities at the science nodes. The method aims at a different objective from existing load management techniques. The proposed algorithm is discussed in Chapter 4.

1.2.4 System Modeling

System modeling and parameter identification are performed in power systems to ensure that the software modules of EMS provide a good representation of the real system. To validate the system models, real measured parameters of the system such as voltages and currents are compared with the ones predicted by the model [23] – [25]. If a model fails to produce a good estimation of the real system parameter, it needs to be tuned by adjusting the parameters of the model [26] – [27]. The updating

process of the model parameters are performed by various numerical techniques such as the Gauss-Newton method [27] and Genetic Algorithm [28]. The targeting models of these methods are usually used to predict the dynamic stability and transients of the system.

The EMS functions of PMACS require a system model in order to provide accurate results that describe system operating conditions. Instead of updating the model to predict transients of the system, parameter identification is used to update the steady state system model. One of the parameters in the system model is the cable resistances of the backbone and spur cables. The cable resistance is considerably larger that the ones in conventional terrestrial power systems at about 1 Ω/km. Due to the high resistance in combination of the physical size of the system, the voltage drop between the nodes is significant. A small variation in per unit resistance can potentially lead to an unexpected scenario if the system model does not reflect the change. The incorrect system model can be identified by comparing the power outputs at the shore stations and the loads at the science nodes with the outputs from the power flow model with inputs of voltages at the science nodes. A cable resistance identification module based on the use of quadratic programming is developed to solve this problem. The details are provided in Chapter 5.

1.3 Monterey Accelerated Research System

The Monterey Accelerated Research System (MARS) project, headed by Monterey Bay Aquarium Research Institute (MBARI), is near completion at the time of this writing and is scheduled for 2007 installation [29]. The purpose of MARS is to serve as a test bed for NETPUNE.

The MARS system has one Shore Station and one Science Node as shown in Figure 1.5. There are sea grounds at each end of the system, i.e., the Shore Station and the Science Node). The cable is standard telecommunications cable (Alcatel OALC4, 17

mm diameter core, 1.6 Ω/km) and the backbone communications technology is 1 Gb/s Ethernet. The communication protocol is TCP/IP. The primary communications between the Node Controller and the PMACS uses the Ethernet provided by the Data Communications Subsystem (DCS). There is a secondary serial RS-232 communications channel for use during operations, in the case of a loss of the primary communications system or for maintenance or troubleshooting.

The Shore Station contains a high voltage power supply from Universal Voltronics (±15 kV DC, 1.111 A) with adjustable polarity, shore ground, the Power Supply Controller (PSC), and the PMACS server computer. The server is on the local area network, synchronized by GPS.

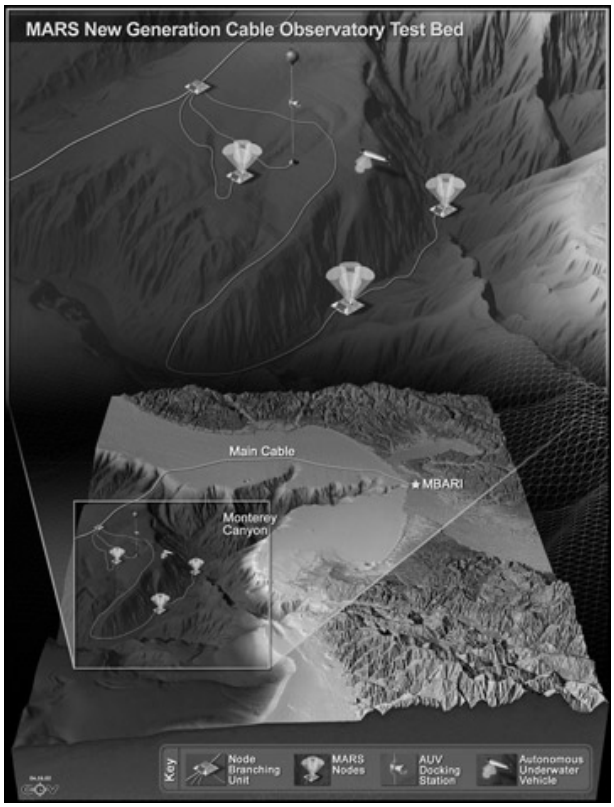

Figure 1.5: The MARS system

The implementation of the MARS PMACS is illustrated in Figure 1.6. The same architecture is used by NEPTUNE. PMACS is constructed with a three-layer client-server architecture. At the lowest layer are the Node Power Controller (NPC) and Power Supply Controller (PSC), in the middle is the PMACS Server, and on top are the PMACS Console and Clients. The NPC is consisted of one CPU board and four analog/digital I/O boards. The PMACS Server is a HP Intel-based server with RedHat Linux.

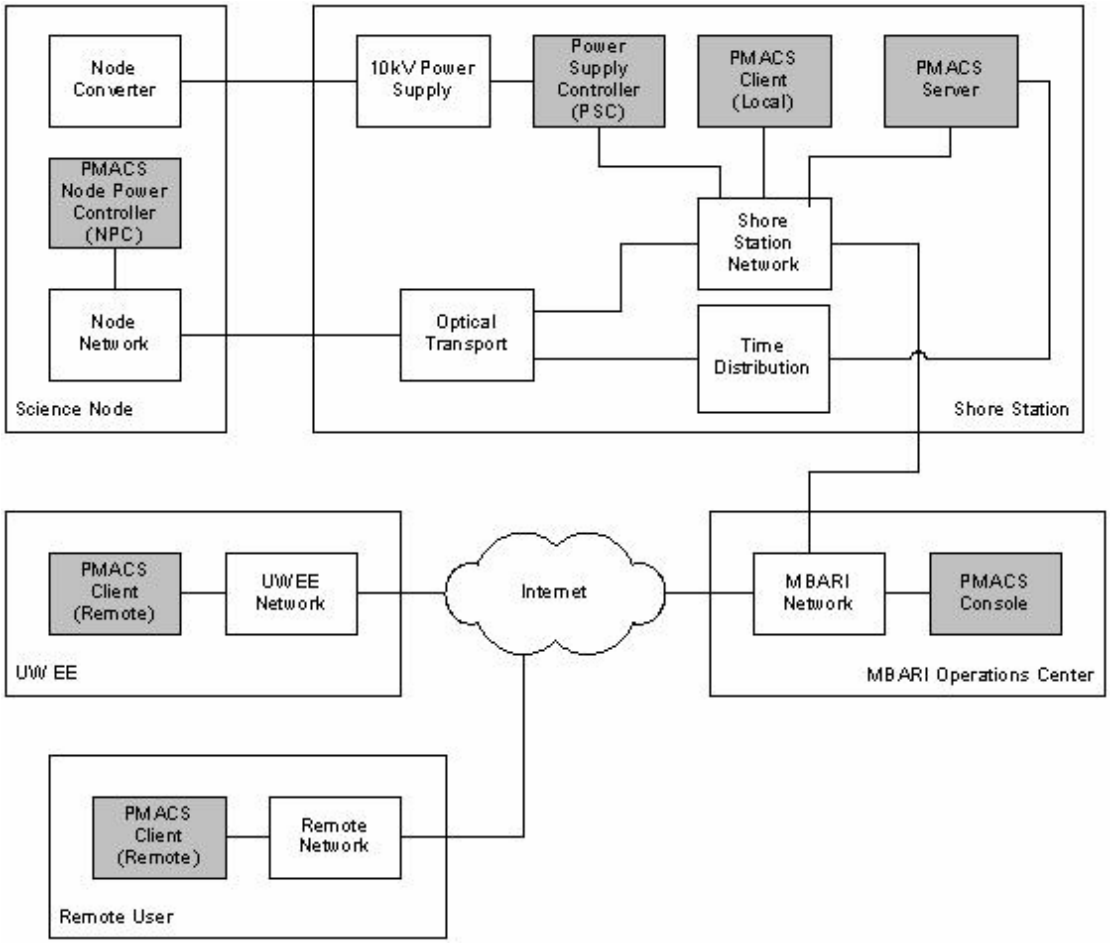

Figure 1.6: MARS PMACS

The Console and Client software is developed using MS Visual Basic.NET. The PMACS Console contains the main user interface for the operator to interact with the actual system, and also provides analytical tools such as the Fault Location and State Estimation module. The main window of the user interface contains a one line diagram of the MARS system. There are also multiple windows to show details of the power subsystem components such as the external loads, internal loads, engineering sensor outputs, converter status, and power supply status. Many of these windows also provide the ability for the operator to control the status of the devices. Figure 1.7 shows the external loads window for the MARS PMACS. There may be multiple Clients but, at any given time, there must be one Console in communication with the Server. The communications between the Console/Client and the Server is using Simple Object Access Protocol (SOAP).

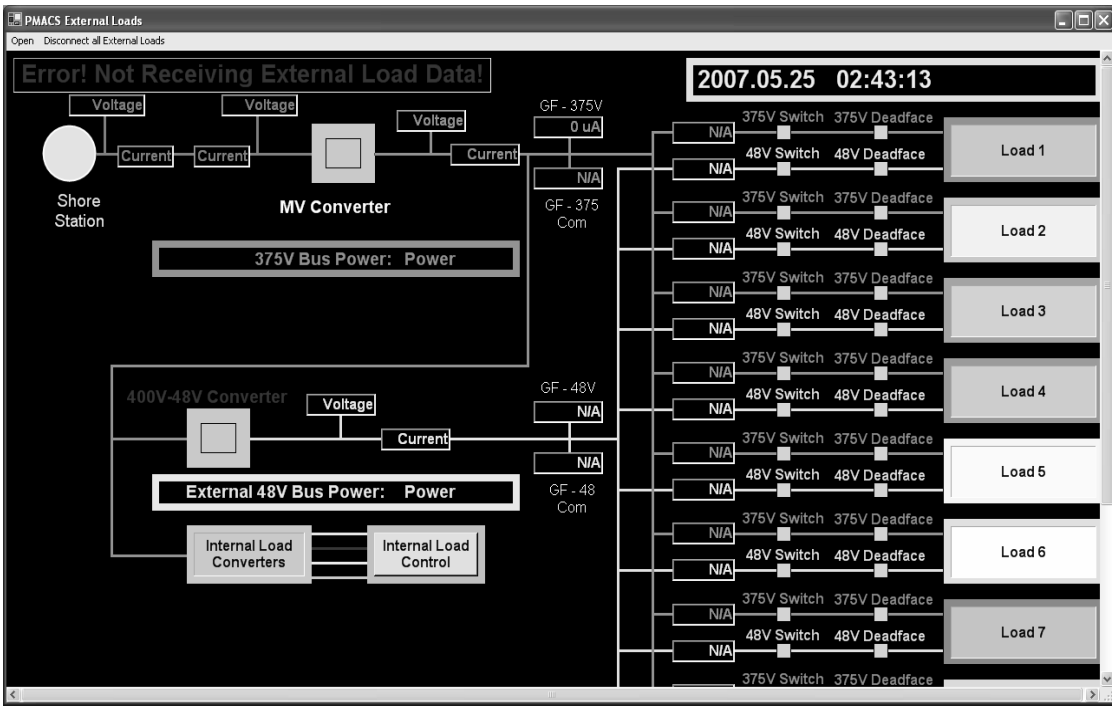

Figure 1.7: MARS PMACS external loads window

The PMACS Server and NPC are able to acquire accurate absolute time-of-day from the DCS. Network Time Protocol (NTP) is used for time-of-day, with an accuracy of approximately 10 msec. The NPC, PMACS Server and PMACS Console are on the same NTP Server to make sure they are all synchronized.

Although the MARS system is much simpler than the planned NEPTUNE system, with only one shore station and one science node, the PMACS architecture and operation philosophy is the same. NEPTUNE and MARS have the same State Estimation and Fault Location modules.

1.3.1 MARS Fault Location Lab Test Results

The Fault Location module of the MARS PMACS uses the same method described in Chapter 3 to estimate the location of a fault on the backbone cable. The communications protocols, devices, and PMACS hardware are the same for both NEPTUNE and MARS. Real-time voltage and current measurements are taken at the Shore Station by the PSC. The PMACS Server sends the data to the PMACS Console for the Fault Location module to perform the calculation.

A lab test has been performed to verify the proposed fault location algorithm using the MARS PMACS software and hardware. Instead of the actual high voltage power supply, a low voltage power supply is used in the lab environment. Instead of the Power Supply Controller, a Node Power Controller with similar functionality and accuracy is used. Resistors are connected in series to simulate the backbone cable. The Node Power Controller measures the input voltage and current. These measurements are acquired by PMACS and processed by the Fault Location module to obtain the (estimated) resistance. The results are shown on the PMACS Console.

The test is conducted at two different voltage levels: 375 V and 48 V. Two different fault scenarios are tested by using 2 different values of resistances: 29.9 Ω and 15.43 Ω. Depending on the type of cable being used in Neptune and MARS, these

values represent the location of the backbone cable fault from the Shore Station. Measurements are taken over a 10 second time span which includes 10 samples. The lab test results are shown in Table I.

The results show that the estimated resistances are within 1 Ω of the actual resistances. These results indicate that the estimated fault location from the proposed algorithm is within 1 km of the actual fault location.

Table I: Fault location lab test results for MARS

Input Voltage	Measured Voltage	Measured Current	Estimated Resistance	Actual Resistance
375V	375.53V	12.48A	29.38Ω	29.90Ω
48V	47.44V	1.62A	29.27Ω	29.90Ω
375V	375.62V	24.18A	15.55Ω	15.43Ω
48V	47.46V	3.17A	14.98Ω	15.43Ω

1.4 Organization of Dissertation

In this dissertation, detailed solutions and algorithm are provided including the general architecture of PMACS and the EMS modules of Fault Location and Load Management. The cable resistance identification module is also included.

The chapters are organized as follows:

Chapter 2 describes the functionalities and features of SCADA system and EMS. The design and architecture of the NEPTUNE is discussed.

Chapter 3 describes the fault location requirement of NEPTUNE and provides details of the formulation and development of the Fault Location Module.

Chapter 4 discusses the issues of management of science node loads and gives a detailed description of the Load Management module.

Chapter 5 deals with the variation of cable resistance and explains how that would lead to a change of system modeling. The problem formulation and technical method of resistance identification are provided.

Chapter 6 summarizes the contribution of this dissertation.

Chapter 2: Power Monitoring and Control System

2.1 Overview of Energy Management Systems

Since the New York Blackout of 1965 power system operators have realized the necessity of coordinated power system operation. A direct result of the 1965 blackout was the emergence of computerized Energy Management Systems (EMS). Due to the available technologies of the time, these systems could perform only a limited number of calculations per second. In order to compensate for this shortcoming in the hardware, software was highly optimized and tailored specifically to a given hardware platform. The result of the software optimization was that the various components of the EMS were so intertwined that they effectively became a single unit.

Figure 2.1 shows the serial manner in which data was handled in the early EMS systems [15]. In addition, it was standard practice to have separate computers run different components of the system. The primary reason for this was that while the network analysis calculations, power flow state estimation, etc., required a large number of floating point calculations, the inputs from the power system meters required a large number of interrupts. These two requirements were incompatible and lead to the use of separate sets of computers, one set for the floating point calculations required for network analysis, another set for SCADA functions capable of a high number of interrupts, and possibly a third for data base functions. The use of various sets of computers compounded the software problems since the code had to be optimized to work with various combinations of computers. The result of these systems, often referred to as Legacy systems, was that piecemeal upgrading or replacement of components of the system was not possible. So by the late 80's, utilities found themselves with outdated hardware that could not be upgraded, resulting in a total, and costly, replacement of the EMS

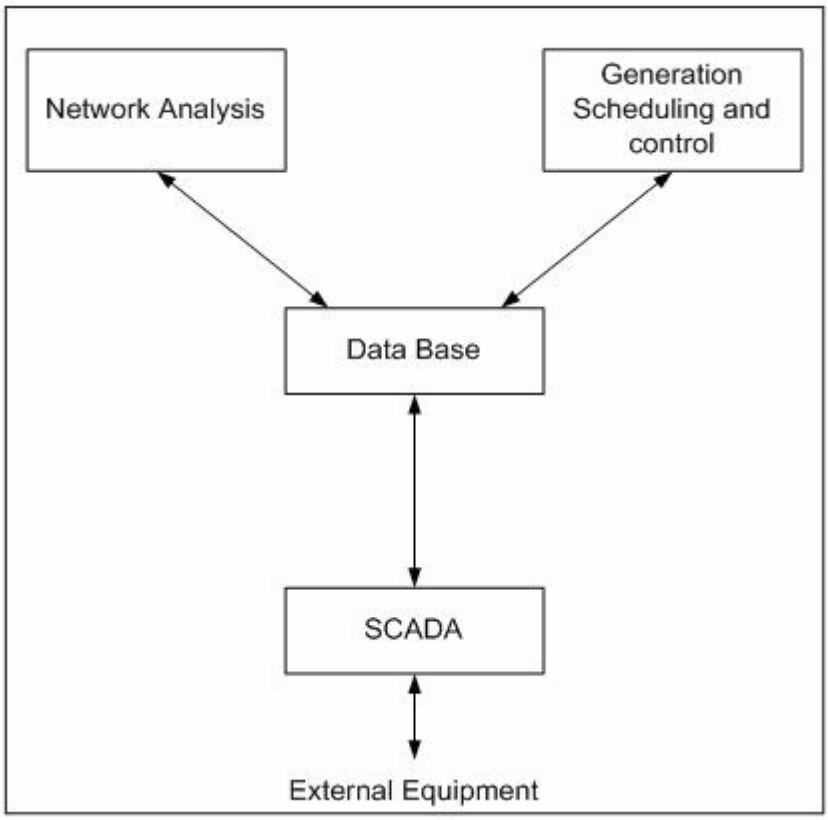

Figure 2.1: EMS architecture 1960's thru late 1980's

Utilities are accustomed to dealing with components with a life span on the order of a few decades. This was not the case with the EMSs systems that would become outdated in less than a decade. This problem was further compounded by the rate at which hardware and software developed during the 80's and 90's. The solution that was offered was an open architecture system. An open architecture system contains 5 key concepts that differ radically from the previous closed architecture systems; portability, interoperability, expandability, modularity, and scalability. Figure 2.2 shows an open architecture of the EMS [16].

- Portability: Refers to ability of the software to run on different software and hardware platforms.
- Interoperability: Refers to the ability to run different software and different

hardware together in the same network.

- Expandability: Refers to the ability to increase the size of the system as well as the scope of the software.
- Modularity: Refers to the ability to add new software functions without adversely affecting the rest of the system.
- Scalability: Refers to the ability to apply the same software to systems of various sizes.

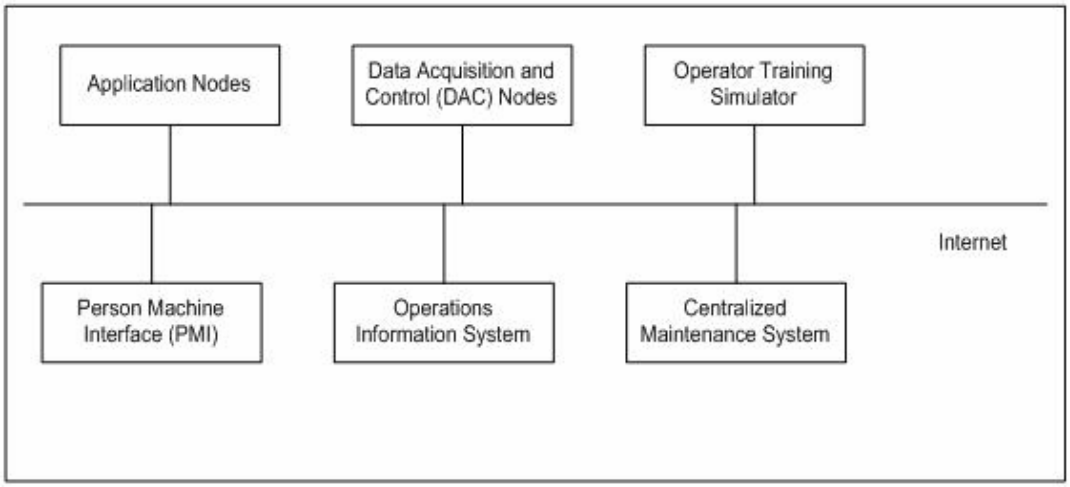

Figure 2.2: Open architecture of EMS

2.2 Overview of PMACS Architecture

NEPTUNE's equivalent of a SCADA/EMS is called the Power Monitoring and Control System (PMACS), which consists of the computer software and hardware that controls and monitors the NEPTUNE power system in a real-time environment. In keeping with the open architecture concepts of Figure 2.2, the top level architecture of NEPTUNE PMACS is shown in Figure 2.3. The power source in the system is the shore station converter located within a facility sited at the Shore Station. The remote location is then connected to Operation Center. From the Operation Center the system

is connected to the Internet via various firewalls. The system can be operated through three distinct locations; the Shore Station, Operation Center, and the University of Washington (UW).

Data from the science node enters the remote site through the data communications subsystem and is routed to the local PMACS computer and to the local RF transmitter/receiver by the L2/L3 switches. The RF link as well as the firewalls will be transparent to the PMACS systems for ease of use.

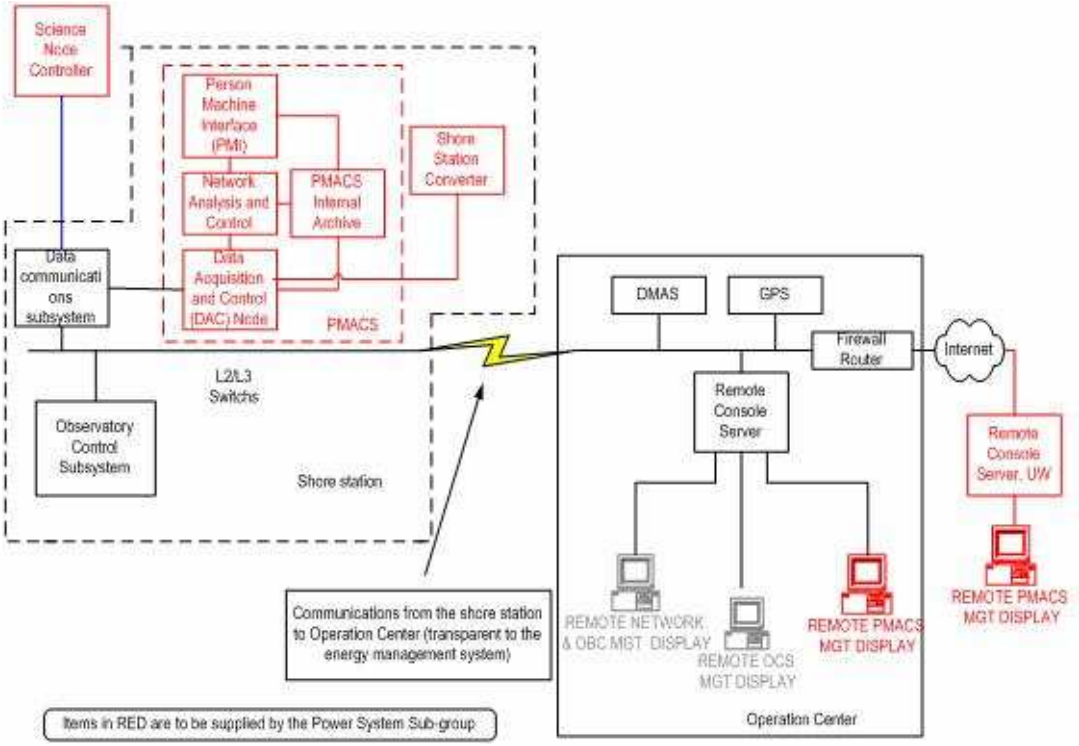

Figure 2.3: Overview of PMACS

PMACS is constructed with a 3-layer client-server architecture as shown in Figure 2.4. The first layer has the Node Power Controller (NPC) and shore Power Supply Controller (PSC) that interacts with the hardware in the science nodes and shore stations. The middle layer is the PMACS Server, which is responsible for collecting

the power system data from science nodes and shore stations, as well as issuing control actions received from the PMACS console; it is the centralized brain of the system. The third layer is the PMACS Console and Client that communicate with the server to gather system parameters such as shore station power supply status, external and internal load status, current and voltage measurements at each bus, converter status and engineering sensor measurements. The PMACS Console displays the system data and is used to perform control actions, such as turning ON/OFF a specific load, through the user interfaces.

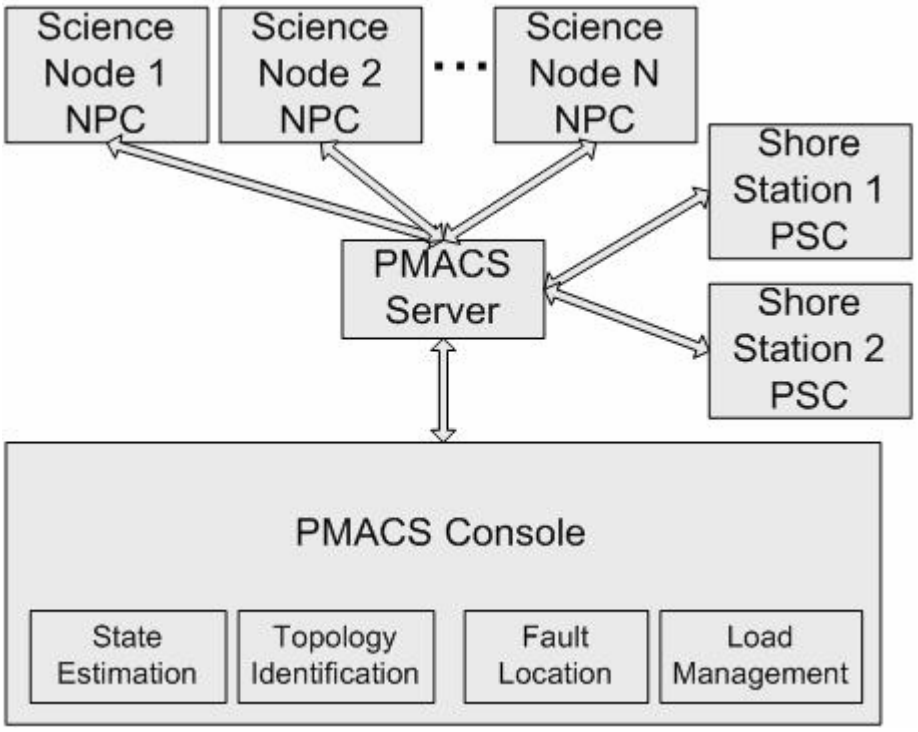

Figure 2.4: Power Monitoring and Control System structure

2.2.2 PMACS SCADA Functions

PMACS has Supervisory Control And Data Acquisition (SCADA) capabilities. (The SCADA system is a standard remote monitoring and control system for electric power systems.) However, PMACS does not have remote control capabilities of the branching unit (BU) breakers since all the protection logics are implemented at the local BU.

According to [17], a SCADA system should have at least one master station and one remote station. It is also common for a system to have several remote stations. For NEPTUNE, there are two ways of implementing the master and remote stations. The first is to have both shore stations serving as sub-master stations and have a third centralized location to be the master station. The science nodes will be the remote stations. In this case, both sub-master stations gather system data and transfer the data to the master station. The communication between the two sub-master systems is also necessary. The master station does not communicate with the remote stations. Another way to implement this is to have both shore stations serving as master stations. One of them is set to be the primary master station and the other one as the secondary master station. The remote stations are the science nodes which gather and transmit data to the masters. Both shore stations need to be able to communicate with each other as well as the remote stations. In the case of a primary master station failure, the secondary master station will take over. The connections between master and remote stations are shown in Figure 2.5.

The master station(s) consists of dual computer systems: the primary computer system and the backup computer system. Both computers are connected to the remote stations through the communications interface. In case of a primary computer system failure, the complete computer system is switched to the backup unit.

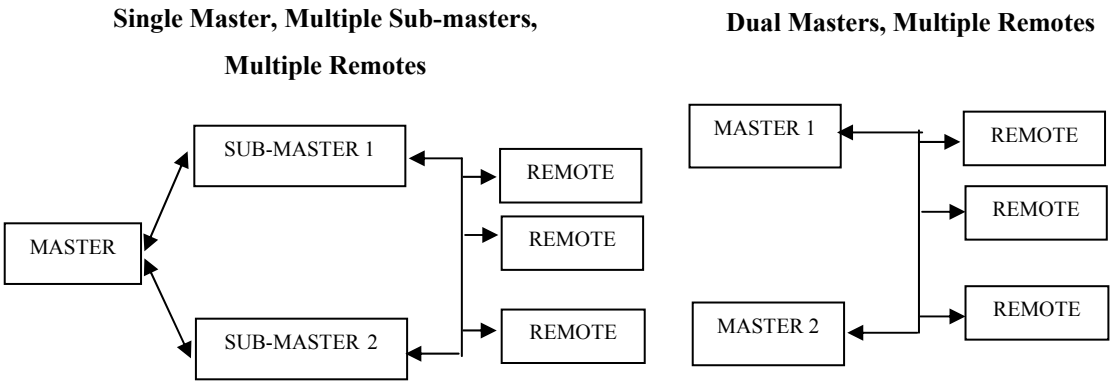

Figure 2.5: Master/remote station interconnections

The man/machine interface (MMI) or person machine interface (PMI) is a standard component of any SCADA system. It is defined as the way an operator interacts with equipment [17]. The interface should include information displays and control capabilities. Information displays can be best represented by a windows-based graphical user interface (GUI) which has a 1-line diagram of the system with multiple levels of details. The user should be able to click on a system component to view detailed information. System components should also be color-coded to indicate the status. In case of an abnormal operating condition of the system, a visual and/or audible indication should be used to alert the operator. The operator should be able to perform standard PMACS functions such as State Estimation and Fault Location through the GUI. Control capabilities of the MMI should include the use of standard windows input devices such as mouse and keyboard. The science nodes are serving as the remote stations. Analog data such as voltage and current measurements as well as digital data such as converter status will be sent to the master station or the sub-master station based on configuration through the communication system every second.

2.3.1 PMACS EMS Functions

PMACS not only serves as a data acquisition system but also an Energy Management System (EMS). Energy Management System functions are performed at the PMACS Console. Outputs will be sent to the PMACS Server and to the MMI for display. The PMACS Energy Management System consists of four separate modules: State Estimation, Topology Identification, Fault Location, and Load Management.

The Fault Location module and Load Management module will be discussed in detail in later chapters of this dissertation.

2.3 PMACS Implementation

PMACS consist of 4 distinct functions; person machine interface (PMI), network analysis and control, data acquisition and control (DAC) node, and the PMACS internal Archive. Figure 2.6 gives an overview of the components of PMACS as well as their associated subcomponents.

2.3.1 Data Acquisition and Control (DAC)

There are two paths for communications in the NEPTUNE system; the primary and secondary systems. The secondary, out-of-band, is little more than a 9600 baud trouble shooting and maintenance system. The primary system is a gigabit Ethernet connection that will normally transmit and receive all of the PMACS telemetered data, as well as science data. While there is only a single fiber path there are conceptually three paths for data to flow into and out of PMACS. Figure 2.7 indicates that all of the data must go through one of the three paths; the command sequence generator, the alert handler, or the data collector. Data can either be

generated on the primary or secondary communications system, in either case the data is processed in the same manner.

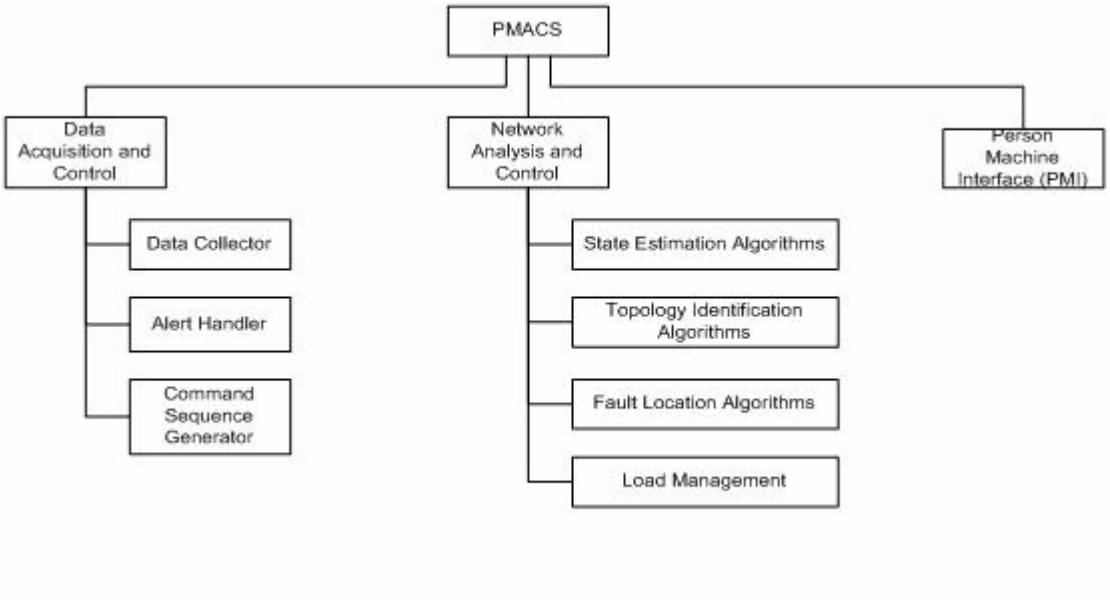

Figure 2.6: Overview of NEPTUNE PMACS components

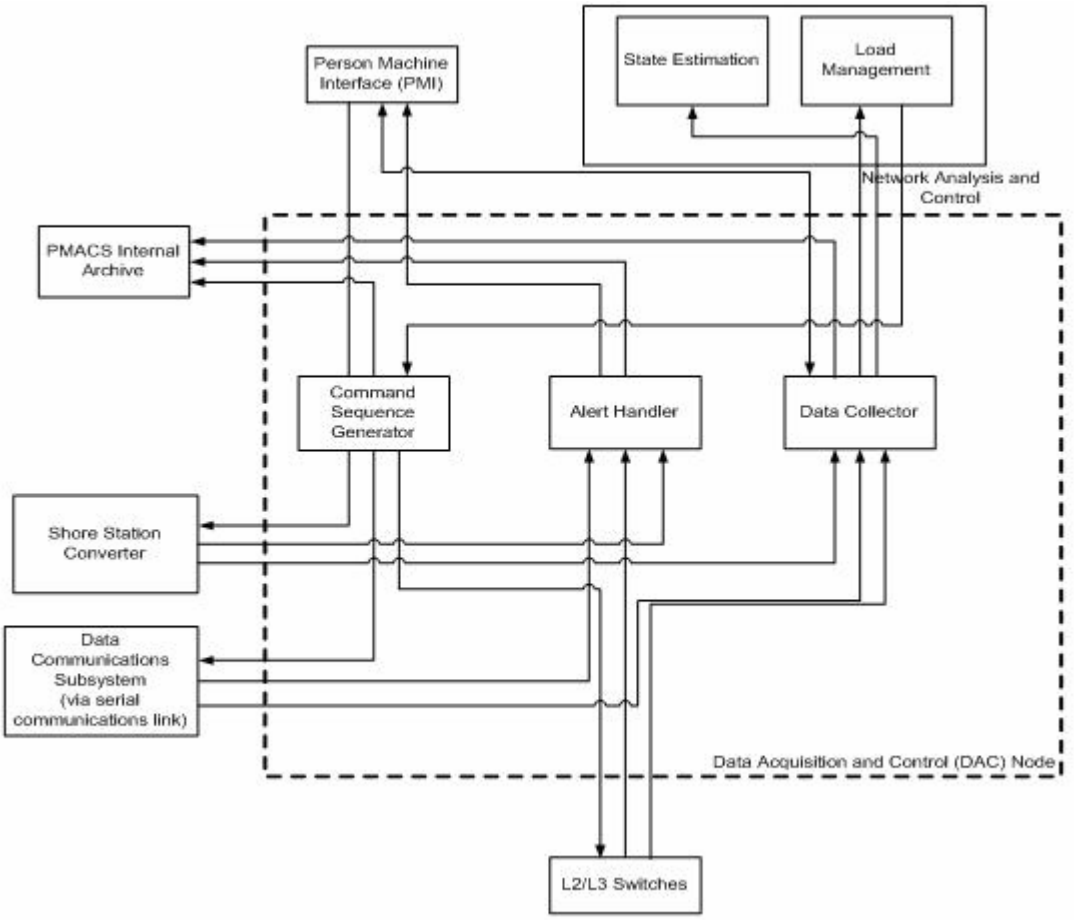

Figure 2.7: Data acquisition and control node

2.3.1.1 Command Sequence Generator (CSG)

The command sequence generator handles all the commands that are generated within the various sections of PMACS. Commands can be generated from the PMI, or the network analysis module. Although the communication system is extremely capable and reliable, it cannot be counted on to be available 100% of the time. Therefore, the possibility must be allowed for that communications will fail during the time a command is being sent to an instrument or a subsystem. The effect of such a failure may be to leave the instrument or subsystem in an unknown or

undesired state. While there are ways to design systems to recover autonomously from loss of communications situations, it is better to guard against unpredictable behavior by sending not commands, but command sequences to the node. The equipment in the node is then programmed not to act until a complete sequence has been received at the node, and its acknowledgement received at shore.

A sequence generator is therefore inserted between the command requests and the communication system. Normally, commands will lead directly to command sequences, and these will be sent forthwith via the communication system. By sending a command sequence instead of simple commands, communications errors can be avoided. The command generator encodes each command with a header and footer and sends it to the appropriate node controller. The node controller will only execute commands that are accompanied by a complete header and footer, thus preventing the execution of partial commands.

All commands that are sent from the command sequence generator are stored in the PMACS internal archive. The command sequence generator is capable of asynchronous communications.

2.3.1.2 Alert Handler

The alert handler is the communications buffer that collects all of the alarms, messages, and other alerts from the science node(s). This data is then passed on to the PMI as well as being stored in the PMACS internal archive. The alert handler is capable of asynchronous communications.

2.3.1.3 Data Collector

The data collector is the communications buffer that collects the power system data from the science node(s) and the shore station converter. The data is then sent to the network analysis and control module as well as the PMI. The data collector polls the data from the science node(s) and shore station converter at a rate that is determined by an input from the user via the PMI, tentatively 1 Hz. The data will be time stamped with a resolution of 1 μs, and the precision is 10 ms.

2.3.1.4 Data Archiving

PMACS will maintain an internal data archive of all system status, parameters, commands, load, schedules, etc. The Node status updates will be synchronously read at a 1Hz rate and all this data will be written to the archive. In addition, all asynchronous data – commands, alerts, schedule changes, etc. – will also be written to the archive. PMACS will maintain 2 internal data archives at 2 different locations – one at the PMACS Server and one at the PMACS Console.

All data that is written to the internal archive will also be transmitted over the network to an external archiving system that can easily be replicated else where. All data will be archived in comma separated ASCII format.

2.3.2 Network Analysis and Control (NAC)

The network analysis and control module is where most of the power system calculations are performed as shown in Figure 2.8. Raw data from the power system is supplied to the NAC via the DAC and operational parameters are input via the PMI.

Commands and system status are then generated and supplied to the DAC, PMI, and the Load Management module as well as being stored in the PMACS internal archive.

Raw data is supplied to the state estimation block which determines the state of the system, including any unknown values. The state variables include the measurements of voltage and current at the nodes. These values, along with the raw data are then used to determine the correct topology of the system. Since state estimation requires knowledge of the correct system topology there will be feedback loop between the state estimation and topology identification block. In addition it is possible for the topology identification block to generate a variation in the shore station voltage, with approval via the PMI, in order to determine the correct topology of the system.

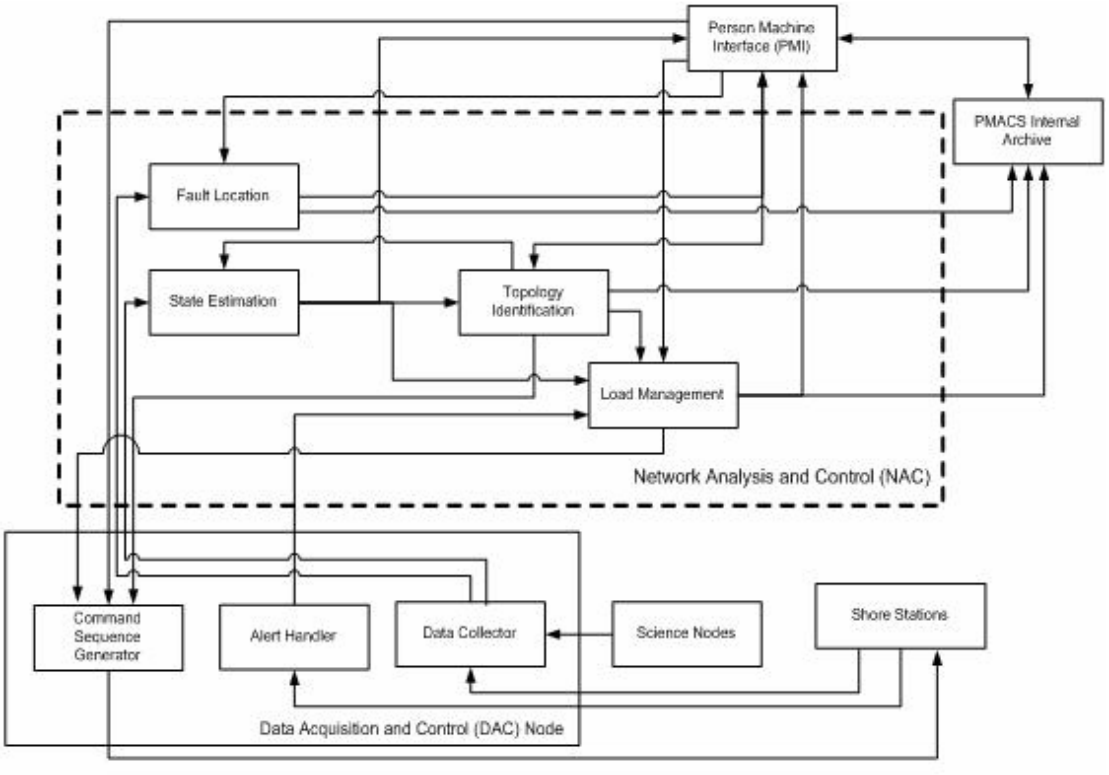

Figure 2.8: Network analysis and control

2.3.3 Person Machine Interface (PMI)

The PMI is duplicated at each of the PMACS control stations; Shore Station, Operation Center, and UW as shown in Figure 2.9. There are three classifications for the operations of the PMI; displayed values, input values, and operator actions.

Displayed values are items such as science node voltage, science node current, low voltage breaker positions, low voltage connector currents, and ground fault indications.

Input values are items such as shore station voltage, backbone low voltage warning level, backbone low voltage limit, backbone low voltage emergency control limit, and backbone high current thresholds.

Operator actions are items such as approval for adjusting shore station voltage level for topology identification and approval for load shedding.

The PMI also allows for the option of performing off-line system analysis such as power flow and dynamic simulation.

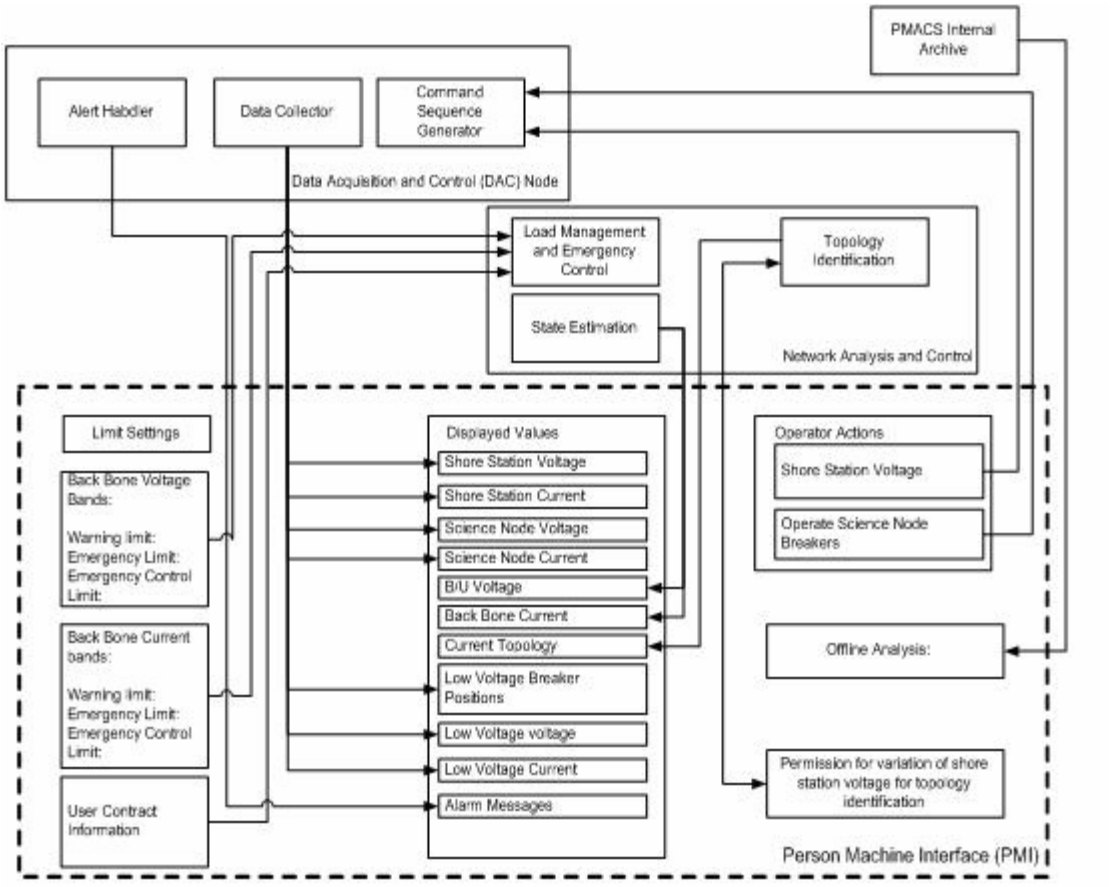

Figure 2.9: PMACS console user interface components

2.4 Summary

In this chapter, the functional description of the Power Monitoring and Control System is presented. The architecture of PMACS consists of the NPC/PSC, Server, and Console. A detailed description is provided for the individual components and modules such as command sequence generator and alert.

Chapter 3: NEPTUNE Fault Location

3.1 Survey of Existing Methods for Fault Location

Traditional power system fault location techniques involve the use of different protection or recording devices, such as Digital Fault Recorders [19], Phasor Measurement Units [20], Digital Relays [30], and Sequence of Events Recorders [31]. Fault locating methods are normally based on transients in voltages and currents measured by these devices. The usage of these types of devices is not feasible for NEPTUNE due to the physical size limitation of branching units and science nodes.

A common method for identifying submarine cable faults is Time Domain Reflectometry (TDR) [21]. The same method is used in underground distribution systems [32]. These applications are used for cable lengths from hundreds of meters to tens of kilometers. Faults on the NEPTUNE power system can be situated 1000 kilometers from the shore. If TDR is used, the reflected signal from the fault would be very weak. Furthermore, the branching unit switches and Zener diodes will also generate a large number of reflected signals which further complicate the process of distinguishing the signal from the noise. Hence, it is determined that TDR is impractical for NEPTUNE due to the attenuation and network configuration of the cable system.

For typical submarine cables, fault location can be conducted by applying voltage and current at one end of the cable into the fault and estimating the resistance of the cable [33]. This method would not work for the NEPTUNE system since it is a networked configuration.

In this research, a new fault location algorithm is derived and implemented for a networked DC power system with low observability. The proposed algorithm makes use of the voltage and current measurements taken at the shore stations. The approach

estimated the location of the fault based on the resistance taken into account the networked system topology

Underwater power systems require a highly accurate fault location technique due to the high cost of repair. The algorithm developed in this research does not require extensive monitoring devices to be installed at various locations on the system. Similar methods may be applied to some terrestrial power systems such as underground distribution systems. Underground distribution systems need to be highly reliable since they are usually located in urban areas with a higher density of load. The difficulty of locating or repairing an underground cable fault is significantly higher than overhead lines. The method described in this paper is a good addition to the existing fault location techniques such as TDR.

The Electric Power Research Institute (EPRI) has a project that uses a similar concept [34] to locate cable faults for rural distribution systems. The research is based on the method described in [35] which uses a Feeder Monitoring System (FMS) to record the voltages and currents on a feeder. This method uses the recorded fault current to compare with a default value stored in a database to estimate the location of a fault based on the feeder impedance.

Impedance-based fault location techniques are used in power systems. The most common impedance-based methods are one-end and two-end methods [36]. The applications are for a single line of AC systems. The method proposed in this paper uses a similar method which is designed for a networked DC system.

3.2 Fault Location Formulation

For the NEPTUNE power system, a backbone cable fault causes the entire system to shut down because of voltage collapse. The system then restarts with the shore station voltage at a low positive voltage, +500 V. During this time, all switches in the BU will close onto the fault. Since the DC-DC converters at the science nodes require

an operating voltage < −5.9 kV, none of the converters will be turned on at the low voltage level of +500 V and, as a result, there is no load or communication in the system. The only circuit carrying currents consists of the backbone cable and the fault in the system. Voltage and current measurements are taken at both shore stations. These measurements will be used by PMACS to determine the fault location. After PMACS takes all the measurements, the polarity at the shore power supply will be reversed (−500 V), a sequence that causes the backbone switches to open and isolate the fault. Service to all loads at the science nodes is then restored [11]-[12] by applying the full −10 kV.

In the fault location mode, all switches will be closed and the fault point is drawing all the current, i.e., there are no other loads. Since communication is not available, the only accessible operating conditions are the voltage and current outputs at the shore stations. PMACS uses these measurements to estimate the total cable resistance and the distances between shore stations and the fault.

To locate a backbone cable fault, several additional factors need to be taken into account:

1) the fault characteristics,
2) fault resistance,
3) topology of the system,
4) cable resistance,
5) voltage drop along the cable,
6) measurement errors.

3.2.1 Fault Modeling

A shunt fault on a submarine cable occurs when the cable's insulation deteriorates, allowing sea water to contact the conductor. Typical causes of shunt faults are:

- Cable is abraded or partially cut. This can occur if the cable is dragged along

the sea floor by a ship's anchor, fishing gear or ocean currents and it sustains cuts and abrasion on the rocky seafloor or outcrops. Trawling is the main cause for this kind of cable fault.

- Cable has a manufacturing flaw such as a void or an inclusion in the insulation.

If the field at that point is high enough, dielectric breakdown can occur.

In most cases, the cable remains a single piece connecting to the ground with some resistance, instead of completely breaking into two separate pieces [33]. The fault on a given link between two Branching Units (BU) can therefore be modeled by the configuration in Figure 3.1.

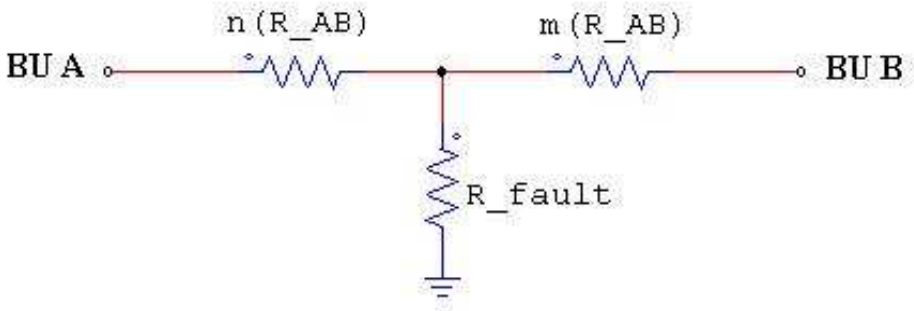

Figure 3.1: Fault model

In Figure 3.1, R_AB is the resistance of the cable link between branching units A and B. R_fault is the *unknown* fault resistance, and *n* and *m* are the *unknown* fractional distances from each of the BUs to the fault location, i.e., $n + m = 1$.

The fault resistance can vary over a range from a few ohms to tens of ohms depending on the condition of the damaged cable and how much conductor is exposed to sea water. This range is based on the findings and experience over years by the author of [33] using a fall-of-potential test.

3.2.2 Component Modeling

It is known that the nominal resistance of the cable is 1 Ω/km or 1.6 Ω/km depending on which of the two types of cable is adopted. Each section will be precisely measured in factory during assembly at a known temperature. However, depending on the actual temperature of the sea water, it could be a few percent lower or higher. There is a temperature coefficient associated with the cable that can be used to calculate the actual resistance based on the temperature of the water (which will likely be available from independent measurements). The estimation of cable resistance can also be done by State Estimation [18], [37].

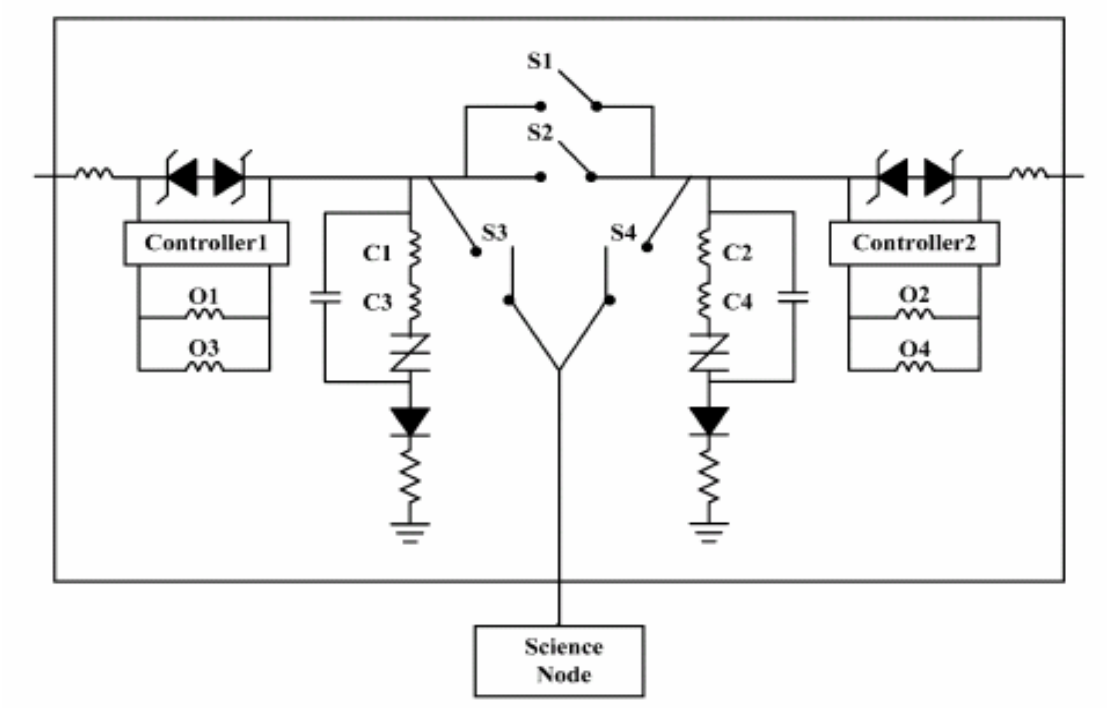

Figure 3.2: Branching unit

Besides the cable resistance, constant voltage drops along each section of the cable need to be considered while locating the fault. Across each repeater on the cable,

there is a voltage drop. Since a BU includes series Zener diodes, as shown in Figure 3.2, there is also a constant voltage drop across each BU. Assuming a BU as shown in Figure 3.2, the voltage drop across the BU is calculated as in (3.1):

$$V_{BU} = 2 \times V_{Zener\,\mathrm{Re}verse} + 2 \times V_{ZenerForward} \tag{3.1}$$

Where:

V_{BU}: voltage drop across a branching unit

$V_{ZenerReverse}$: reverse bias voltage of a zener diode

$V_{ZenerForward}$: forward bias voltage of a zener diode

The zener diode reverse bias voltage is 6.9V, and the forward bias voltage is 0.7V. Therefore, the voltage drop across one BU circuit is 15.2V. The voltage drop across a repeater is 7.6V. The total voltage drop for each section of the backbone is the sum of the repeater voltage drop and the BU voltage drop.

3.2.3 System Modeling

As mentioned, the minimum operating voltage for the DC/DC converters in the science nodes is -5.9 kV; therefore, there is no load in the system during fault location except the fault itself. Since all switches will be closed onto the fault, the topology of the entire system is known when taking the measurements. The fault is not isolated until all measurements are taken.

Since the system is a meshed network, currents converge to the fault point through multiple paths. Since the system topology is known, the equations for each path can be written taking into account the unknown currents, and known cable resistances and voltage drops. Figure 3.3 shows the system topology with node and link numbers.

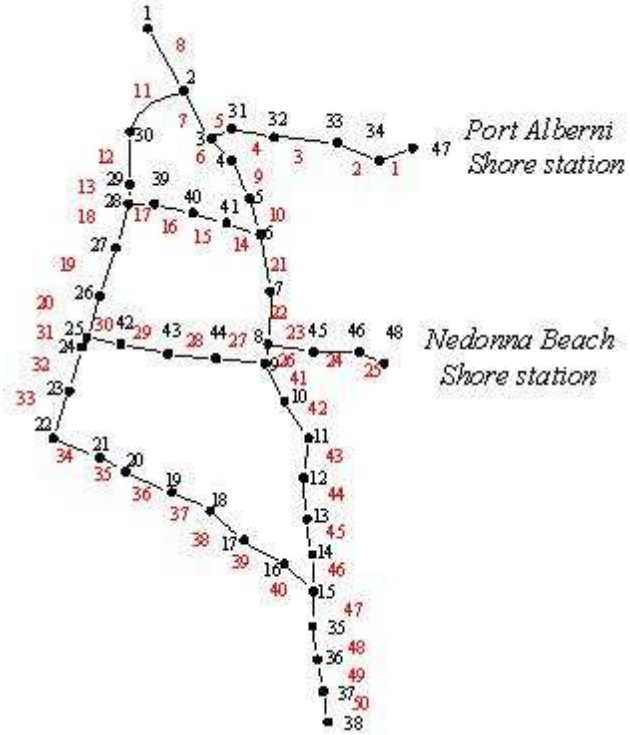

Figure 3.3: System topology with node and link numbers

3.2.3.1 Generalization

For a system with a meshed structure, each branch corresponds to an unknown current. A fault from a line to ground is also modeled as a branch. For a system condition under which no external load is connected, the fault current is known and it is the sum of all input currents.

For a system with multiple sources, multiple equations can be written based on the circuit parameters and the current flowing through each path. For a Y-shape branch, there are a total of three currents, but one of them can be expressed as the sum or difference of the other two. When there is no external load, 1/3 of the branch currents can be expressed in terms of a known current and another unknown current(s). This procedure reduces the total number of unknowns in the system to 2/3 of the number of

unknown currents plus the addition of the fault resistance and faulted section cable resistance. For a fault on a system with multiple sources to be determined, the total number of paths from the sources to the fault should be larger than or equal to the total number of unknowns for any given fault in the system.

Based on the result from the previous paragraph, the total number of unknowns for the NEPTUNE system is 7, i.e., fault resistance, faulted cable resistance fraction *n*, and the number of unknown currents on different paths. There are 2 sources and the number of available paths from the 2 sources to anywhere in the system is larger than 7. Therefore, all fault locations on the NEPTUNE system are well specified. The equations for the paths can be written in the following general form (3.2):

$$V_{SSi} = \sum_{p_{ij}} (I_{p_{ij}} R_{p_{ij}} + V_{D_{p_{ij}}}) + \frac{1}{2} V_{D\_faulted\_link} + I_{faulted\_link} n R_{faulted\_link} + I_f R_f \tag{3.2}$$

where:

$V_{SS\,i}$: Voltage outputs of Shore Station i, i = 1, 2

P_{ij} : j th path from shore station i to the fault, i=1, 2

I_{pij} : Currents on links of the path

R_{pij} : Cable resistance of the links of the path

V_{Dpij}: Voltage drop across links of the path

$V_{D\_faulted\_link}$: Voltage drop across the faulted link

$I_{fault\_link\backslash}$: Current on the faulted link

n: Per unit distance of the faulted link

R_{fault_link}: Cable resistance of the faulted link

I_f: Fault current

R_f: Fault resistance

In the proposed formulation, the current direction is assumed to be from the shore station toward the fault. The equations needed are chosen based on the *shortest distance paths* from each shore station to the faulted link. Current directions on the shortest path will apply to the next paths identified for loop analysis. Since the cable resistance is associated with an error, the shortest cable length would introduce the smallest error. In PMACS, the paths are identified automatically by shortest-path search.

3.2.3.2 System Modeling for NEPTUNE

Now suppose a backbone cable fault is present on cable link 9 between nodes 4 and 5. The voltage and current measurements from both shore stations are given. Since the topology is known, the loop equation from each shore station to the fault can be written. For the loop equations, path P_{11} includes cable links 1, 2, 3, 4, 5, and 6 and path P_{12} includes cable links *25*, 24, 23, 22, 21, and 10. Each equation is non-linear with unknown currents as in (3.3) and (3.4). The non-linearity is due to the nature of the Zener diodes in the system.

$$\begin{aligned} V_{SS\,1} &= I_1 R_1 + V_{D\,1} + I_2 R_2 + V_{D\,2} + I_3 R_3 + V_{D\,3} \\ &\quad + I_4 R_4 + V_{D\,4} + I_5 R_5 + V_{D\,5} + I_6 R_6 + V_{D\,6} \\ &\quad + \frac{1}{2} V_{D\,9} + I_{9'} n R_9 + I_9 R_f \end{aligned} \tag{3.3}$$

$$\begin{aligned} V_{SS\,2} &= I_{25} R_{25} + V_{D\,25} + I_{24} R_{24} + V_{D\,24} + I_{23} R_{23} + V_{D\,23} \\ &\quad + I_{22} R_{22} + V_{D\,22} + I_{21} R_{21} + V_{D\,21} \\ &\quad + I_{10} R_{10} + V_{D\,10} + \frac{1}{2} V_{D\,9} + I_{9''} m R_9 + I_9 R_f \end{aligned} \tag{3.4}$$

where:

$V_{SS\,i}$: Voltage outputs of Shore Station i, i = 1, 2

I_k: Current on link k, k = 1…50

$V_{D\,k}$: Voltage drop across link k, k = 1…50

$I_{9'}$: Current on link 9 from Node 4 to fault

I_9 : Current on link 9 from Node 5 to fault

m, n: Per unit distance of Link 9

R_f: Fault resistance

The faulted link can be expressed in per unit length such that:

$$nR_{fault\_link} + mR_{fault\_link} = R_{fault\_link} \tag{3.5}$$

Additional non-linear equations need to be written by loop analysis from the shore stations to the fault via the *next shortest paths* from shore stations 1 and 2, respectively, as shown in (3.6) and (3.7).

$$\begin{aligned} V_{SS1} = {} & I_1R_1 + V_{D1} + I_2R_2 + V_{D2} + I_3R_3 + V_{D3} \\ & + I_4R_4 + V_{D4} + I_5R_5 + V_{D5} + I_7R_7 + V_{D7} \\ & + I_{11}R_{11} + V_{D11} + I_{12}R_{12} + V_{D12} + I_{13}R_{13} + V_{D13} \\ & + I_{17}R_{17} + V_{D17} + I_{16}R_{16} + V_{D16} + I_{15}R_{15} + V_{D15} \\ & + I_{14}R_{14} + V_{D14} + +I_{10}R_{10} + V_{D10} \\ & + \frac{1}{2}V_{D9} + I_{9''}mR_9 + I_9R_f \end{aligned} \tag{3.6}$$

$$\begin{aligned} V_{SS2} = {} & I_{25}R_{25} + V_{D25} + I_{24}R_{24} + V_{D24} + I_{23}R_{23} + V_{D23} \\ & + I_{22}R_{22} + V_{D22} + I_{22}R_{22} + V_{D22} + I_{21}R_{21} + V_{D21} \\ & - (I_{14}R_{14} + V_{D14}) - (I_{15}R_{15} + V_{D15}) - (I_{16}R_{16} + V_{D16}) \\ & - (I_{17}R_{17} + V_{D17}) - (I_{13}R_{13} + V_{D13}) - (I_{12}R_{12} + V_{D12}) \\ & - (I_{11}R_{11} + V_{D11}) - (I_7R_7 + V_{D7}) \\ & + I_6R_6 + V_{D6} + \frac{1}{2}V_{D9} + I_{9'}nR_9 + I_9R_f \end{aligned} \tag{3.7}$$

Note that all link currents are unknowns; however, since there is no load during fault location, shore station currents are feeding the fault point. Therefore:

$$I_{SS1} + I_{SS2} = I_9 \tag{3.8}$$

where:

I_{SSi}: Current outputs of Shore Station i, i = 1, 2

From the topology of the system, it can be seen that:

$$I_{SS1} = I_1 = I_2 = I_3 = I_4 = I_5 \tag{3.9}$$

$$I_{SS2} = I_{23} = I_{24} = I_{25} \tag{3.10}$$

$$I_7 = I_{11} = I_{12} = I_{13} = I_{SS1} - I_6 \tag{3.11}$$

$$I_{14} = I_{15} = I_{16} = I_{17} = I_{9''} - I_{21} \tag{3.12}$$

Similarly, the current of any other link can be written as an expression of the known currents I_{SS1}, I_{SS2} and some unknown current(s). Substitute (3.9-3.12) into (3.3), (3.4), (3.6), and (3.7), the number of unknowns in the equations is reduced. The number of non-linear equations needed to solve a fault on a specific link is different for each link.

The number of non-linear equations should be 1 less than the number of unknowns since there is an unknown fault resistance. However, with the addition of (3.5), there is an equal number of equations and hence the solution can be found by numerical techniques. MATLAB is used to solve the non-linear equations for the values of m and n.

3.3 Worst Case Analysis

When taking the voltage and current measurements at the two shore stations, each of them is subject to error. This error affects the result of the estimated resistance and hence the estimated fault location. To reduce the error effect, multiple independent measurements should be taken at shore stations.

Assume that the line resistance is 1 Ω/km. Since the goal is to locate the fault to within ±1 km, the error in terms of resistance should be within ±1Ω. If the error in resistance for the worst case can be contained within ±1Ω, the error in fault distance would be smaller than ±1 km for any other cases. In this study, a worst case analysis is conducted to determine the maximum allowable voltage and current measurement errors.

Note that the *worst case* resistance as a random variable and its *variances* are given by:

$$\frac{V_1}{I_1} = R_{\max}$$

$$\sigma^2_{R_{\max}} = \sigma^2_{V_1}\left(\frac{\partial R}{\partial V_1}\right)^2 + \sigma^2_{I_1}\left(\frac{\partial R}{\partial I_1}\right)^2 + 2\sigma_{V_1 I_i}\left(\frac{\partial R}{\partial V_1}\right)\left(\frac{\partial R}{\partial I_1}\right)$$

where:

$$\left(\frac{\partial R}{\partial V_1}\right) = \frac{1}{I_1}$$

$$\left(\frac{\partial R}{\partial I_1}\right) = -\frac{V_1}{I_1^2}$$

$$\sigma^2_{R_{\max}} = \sigma^2_{V_1}\left(\frac{1}{I_1}\right)^2 + \sigma^2_{I_1}\left(-\frac{V_1}{I_1^2}\right)^2 + 2\sigma_{V_1 I_i}\left(\frac{1}{I_1}\right)\left(-\frac{V_1}{I_1^2}\right)$$

$$\sigma^2_{R_{\max}} = \frac{\sigma^2_{V_1}}{I_1^2} + \frac{\sigma^2_{I_1} V_1^2}{I_1^4} - \frac{2\sigma_{V_1 I_1} V_1}{I_1^3}$$

Now assume a *non-worst case* $R < R_{max}$, V_1 remains the same since it is the shore station output voltage and hence the non-worst case current $I_1' > I_1$.

$$\frac{V_1}{I_1'} = R$$

$$\sigma_R^2 = \sigma_{V_1}^2\left(\frac{1}{I_1'}\right)^2 + \sigma_{I_1}^2\left(-\frac{V_1}{(I_1')^2}\right)^2 + 2\sigma_{V_1 I_1}\left(\frac{1}{I_1'}\right)\left(-\frac{V_1}{(I_1')^2}\right)$$

$$\Rightarrow \sigma_R^2 < \sigma_{R_{max}}^2$$

Using the values for the NEPTUNE system, it is found that the worst case is a fault on link 50 since the cable resistance and voltage drops are both the largest among all fault scenarios. This analysis suggests that if the algorithm can locate a fault on link 50 within ±1 km, it should locate any other fault on the NEPTUNE system within better than ±1 km.

3.4 Voltage Level Requirements

As mentioned, when a fault occurs, the system shuts down and then restarts with a positive voltage. The Zener diodes have a knee current of about 150 mA. In this region, the voltage drop is proportional to the current (and hence is not constant). Due to the nature of the system, some currents on the branches might be very small. Since there is no communication during the fault location mode, the currents on the branches are unknown. Therefore, voltage outputs at the shore stations need to reach a sufficient level to ensure that all currents on the branches are large enough so that the Zener diodes will have constant voltage drops. The shore station voltage requirements vary when a fault is located on different links. For a fault on a specific link, there is a required minimum voltage to locate the fault to within 1 km. There is also a maximum voltage level for each specific scenario since the maximum current allowed on a

backbone cable should not exceed 10A. If the voltage at the shore station is higher than the maximum allowable level, the backbone current exceeds 10A somewhere in the system.

During restarting, sometimes voltage and current measurements for fault location are taken before the system goes back to normal operation. In this case, the faulted link is not known at the point when measurements are taken. Therefore, the voltage levels to apply at the shore stations cannot be determined. Instead, current outputs at the shore stations are raised until the sum of the two currents is close to 10 A. This ensures that Zener diodes are operating in the saturated region, and the constraint of 10 A is not exceeded.

If the system operator decides to go back to normal operation without taking fault measurements and come back for the measurements at a later time, the faulted link can be identified before the measurements are taken. In this case, the system can apply a voltage level that would guarantee the sufficient level of current in the branches without violating the current limit. Figure 3.4 shows the minimum and maximum allowable voltage levels necessary to resolve a fault location on a given link to the desired accuracy.

Notice that link 1 and link 25 are connected to the shore stations. If the fault is located close to the shore station, even a small voltage might result in a high current. Since the true fault location is not known, the maximum voltage level can not be used in order to avoid a current that exceeds 10 A. Instead, the voltage at the shore stations is increased until the current reaches 5 A. The corresponding voltage and current measurements are then used to perform the fault location.

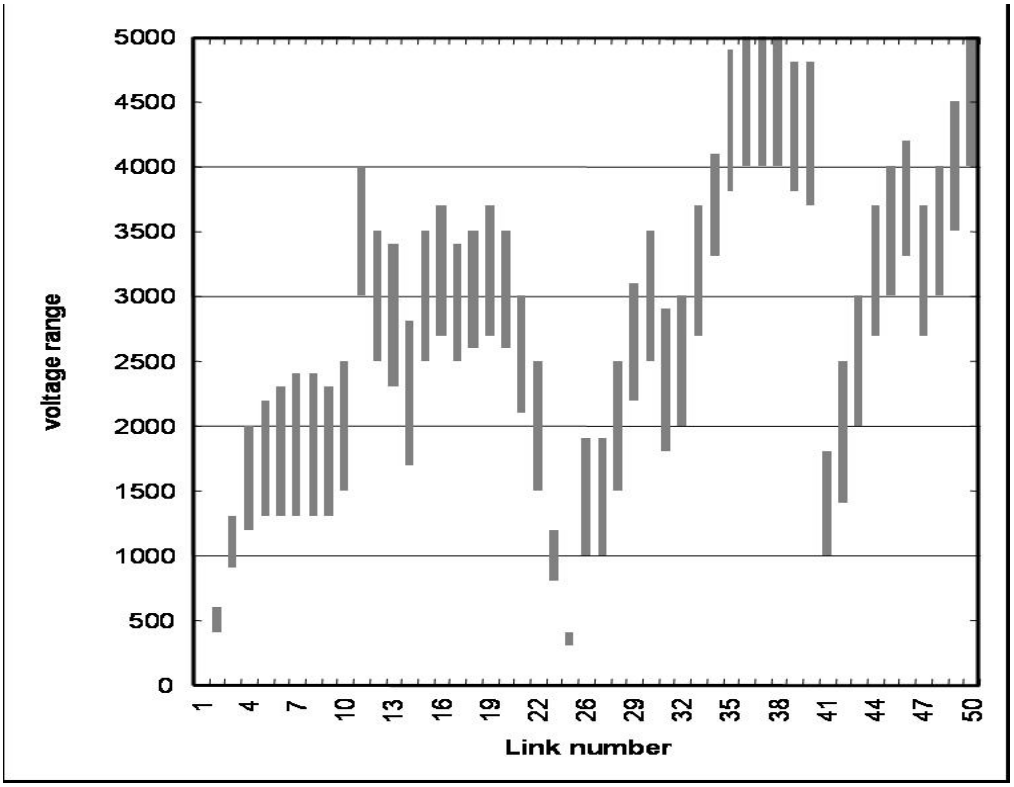

Figure 3.4: Voltage requirements

3.5 Simulation Results for the NEPTUNE System

The first step to estimate the fault location for the NEPTUNE power system is to formulate the set of non-linear equations similar to (3.3) and (3.4) for the proposed topology shown in Figure 3.3. Port Alberni is Shore Station 1, and Nedonna Beach is Shore Station 2. For a given fault, the fault location algorithm constructs the non-linear equations based on the discussion in Section 3.2.3.2. The faulted link can be identified by the algorithm described in [38]. Although the constant voltage drops on the cable sections are not shown on the figure, their values are taken into account when formulating the equations. The number of equations required to solve for the fault location depends on the specific faulted link.

Table II shows some results of simulated cable faults on different links with different fault resistances. A normally distributed random error of zero mean and 0.01% standard deviation is added to the voltage and current shore station measurements. The calculation has been performed 30 times simulating 30 sets of independent measurements.

Table II: Fault location results for NEPTUNE

Faulted Link	**Faulted Location**	**Fault Resistance**	**Estimated Fault Location**
9	20km from Node 4	2Ω	19.5km from Node 4
12	40km from Node 30	1Ω	39.7km from Node 30
16	25km from Node 40	2Ω	24.2km from Node 40
22	71km from Node 7	1Ω	71.6km from Node 7
28	10km from Node 44	1Ω	10.8km from Node 44
35	40km from Node 21	3Ω	38.6km from Node 21
44	20km from Node 12	3Ω	20.8km from Node 12
50	50.8km from Node 37	0Ω	49.9km from Node 37

Assume that a fault is presented at the far end of link 50 to represent the worst case scenario. When both shore stations have a voltage output of 4300 V, I_1 is 1.51 A and I_2 is 4.33 A. A normally distributed random error of zero mean and 0.01% standard deviation is added to these simulated voltage and current measurements. The calculation was performed 30 times simulating 30 sets of independent measurements. When solving the non-linear equations, it yields an average solution of $n = 0.9958$ and $m = 0.0042$. Since the line segment is 215 km long, the error in estimating the fault location is m times 215 or 0.9 km. Therefore, it shows that 4300 V from both shore stations would be a sufficient voltage level to handle the worst case. For faults in different locations in the system, the voltage level does not exceed 4300 V.

As shown in Table II, the estimated fault location is very close to the actual location in most cases. The only case where the algorithm does not meet the 1 km requirement is the cable fault on Link 35, with an error of 1.4 km. This could be due to the fact that Link 35 is very far from both shore stations yielding large errors in measurements and the fault resistance is larger than other cases.

3.6 Software Implementation of the Fault Location Module

As shown in Figure 3.5, the implementation of the proposed fault location algorithm for PMACS requires the following information as shown in Figure 3.5:

1) faulted link identity,

2) real-time voltage and current measurements from both shore stations, and

3) system topology.

The faulted link will be identified by the Topology Identification module of PMACS. PMACS will set the voltage levels for the shore stations and measure the current outputs. The topology is stored in a database. Once the NEPTUNE system restarted after a shutdown due to a fault, the PMACS Fault Location module will apply the knowledge of the system topology combined with the measurements from the shore station and the algorithm described in the previous sections to identify the location of the backbone cable fault. Once the fault is located, PMACS will adjust the shore station voltage outputs to -500 V so that the fault will be cleared by the switches in the Bus and the system can be restored to normal operations. During these operations, the PMACS Console is only able to receive data and send command to the shore stations.

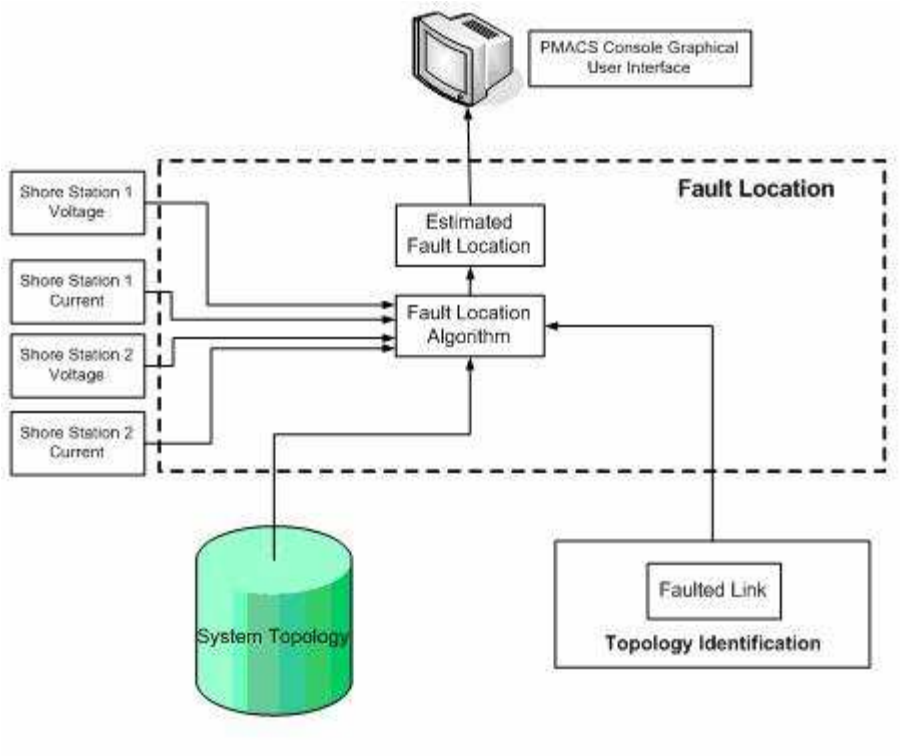

Figure 3.5: Fault location implementation for PMACS

In this study, a software module has been developed for the fault location function. Figure 3.6 shows the PMACS user interface for the Fault Location module for NEPTUNE. Currently, the shore station measurements are generated by simulated data. The measurements are processed by the fault location algorithm software. The estimated fault location is displayed through the user interface.

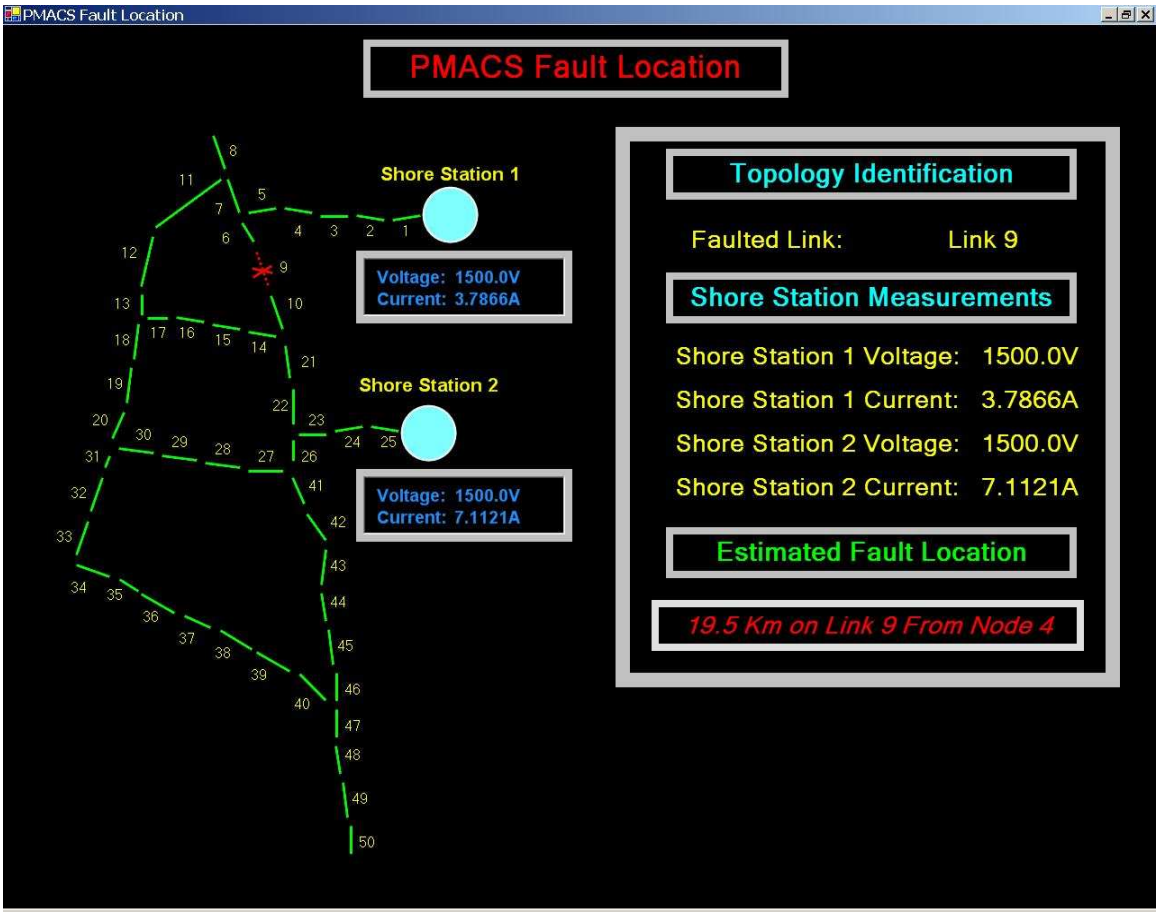

Figure 3.6: PMACS user interface for fault location

3.7 Summary

The algorithm developed in this chapter is a full scale version of the resistance estimation method that is used in point-to-point underwater applications. The algorithm applies the available voltage and current measurements from the shore station to identify the location of a backbone cable fault. It has the ability to locate a cable fault in a meshed configuration and does not have the limitation of cable length as it does for the TDR method. The same algorithm may also be applied in underground cable systems or HVDC systems.

Chapter 4 Neptune Load Management

4.1 Introduction

For conventional power systems, the goals of load management are normally to reduce the operational cost or increase reliability margin of the system [22], [39]-[41]. However, for the NEPTUNE power system, the purpose of the Load Management module of PMACS is to determine the maximum amount of load the system can serve without violating any system constraint. Even though current battery operated oceanographic equipment often requires less than 1 W, it is expected (and hoped) that the nominal 10 kW at a node will be quickly utilized for lighting (e.g., for high definition video), battery charging (autonomous undersea vehicles), pumping of water (high volume chemical sampling), and acoustics systems (navigation, communications and tomography). Thus, managing the limited resource of power given the various constraints will likely be an immediate challenge.

The total power the system can provide is limited by the maximum voltage output of the power supplies as well as the current limit on the backbone cables. The nominal voltage output of the power supply at each shore station is 10 kV. The backbone cables have a nominal 10 A current limit. Therefore, the maximum total power the system can provide at any given time is 200 kW. Each individual science node can consume up to 10 kW. A portion of the power is to be used to supply the communications devices at the science nodes which are the internal loads. Assuming the power delivered to the internal loads is 1000 W, the peak power delivered to science users is 9 kW at each science node. It is clear that the system would not be able to simultaneously supply the maximum load at every science node.

In the NEPTUNE power system, the amount of power being delivered to the external loads at science nodes is defined by contracts with the science users. The user

contract provides specifications of the load including the nominal amount of power the load is to consume as well as the priority of the load. Should the user's equipment develop a fault so that the power demand exceeds the agreed amount, control should be taken to limit the power. PMACS will determine if power consumption should be limited using the acquired data. A related effort is the disconnection of users in the event that the power, a limited resource, is to be reserved for high-priority applications. For example, it may be decided that priority should be given to lights and removed from battery recharging when some sudden underwater event such as an earthquake is detected. To disconnect the users, PMACS identifies the appropriate switches to open so that service to other loads will not be disrupted. PMACS maintains a list of priorities of the loads and uses the information on power consumption and the agreement between NEPTUNE and users to determine whether it is necessary to shed load. Based on the power available, PMACS identifies load devices that need to be shed for the operating condition. There are three levels of priorities: high, medium, and low. The system will try to serve the loads at a higher priority before attempting to serve loads at a lower priority. It is assumed that the complexities of sensor networks (e.g., tree and mesh structures) beyond the primary science nodes are unimportant here. Note that over-current conditions resulting from a fault should be handled by the protection system. The task of the Load Management module in PMACS is to handle high currents due to overloading.

In the current design of NEPTUNE, the length of the backbone cable between each of the BUs ranges from tens of kilometers to over a hundred kilometers. The lengths of spur cables would be several to tens of kilometers. Typical cable resistance is 1-1.6 Ω/km. Since the resistances of long cable sections are not small, the voltage drops from the shore stations to the remote locations will be significant. If the current on a 100 km backbone cable between 2 nodes equals 1 A, the voltage drop between the nodes would be 100 V if the cable resistance is 1 Ω/km. Each DC-DC converter at the science nodes has an internal control loop to regulate its own load voltage.

However, the DC-DC converters serving the loads can not operate if the input voltage drops below (in absolute value) 5.9kV. Hence, PMACS must be able to monitor node voltages and determine if it is necessary to raise or drop source voltages and/or drop load so that the entire voltage profile along the cable system remains within an acceptable range at all times. A voltage profile is illustrated in Figure 4.1. One of the constraints of the Load Management algorithm is to ensure that voltage levels at all science nodes are within range.

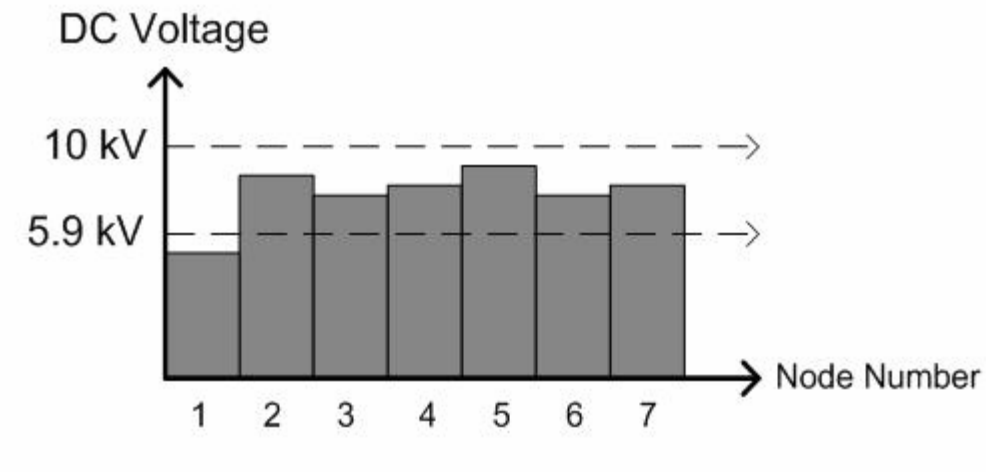

Figure 4.1: Voltage profile with limits

In a similar manner, PMACS must monitor the current profile along the backbone. The current limit used for the backbone cable is 10A. In a normal condition, over-current would not occur. However, if one of the shore stations is out of service and all loads are served from the remaining shore station, load currents will increase significantly for some sections of the backbone, particularly those sections close to the shore station in service. The Load Management module takes into account the current limit as one of the constraints and determines the new optimal operating condition when the system topology is changed.

4.1.1 Operation Modules of Load Management

The Load Management of PMACS can be divided into three operation modules for different aspects of the system. The goal is to deliver the maximum power while satisfying all the constraints under various scenarios: real-time, planning, and system restore. Three different modules as shown in Figure 4.2 are defined to handle different scenarios of the NEPTUNE power system. The control capabilities of PMACS enable the system to regulate itself under abnormal operating condition so that it would reach its sub-optimal state by delivering the maximum amount of power to the science users.

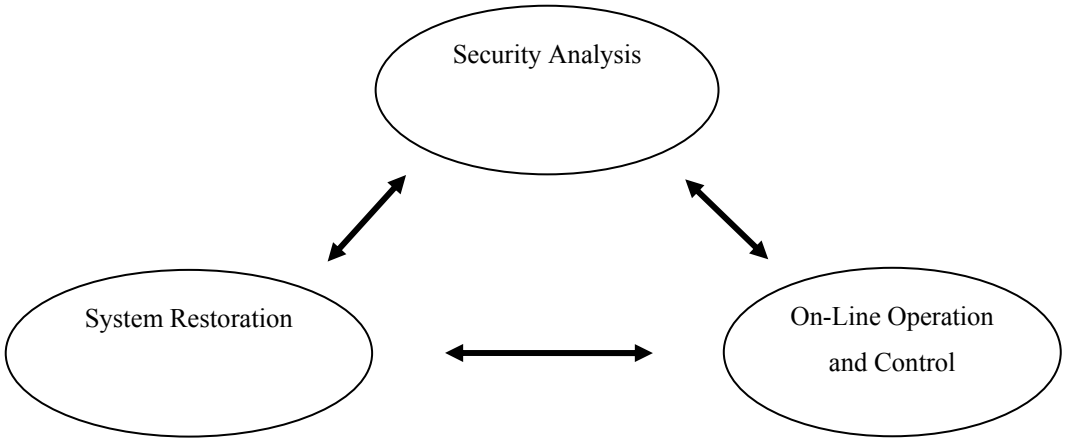

Figure 4.2: Load management modules

4.1.1.1 Security Analysis

The power consumption of any science user is limited by a user contract. When a science user request to turn on the load at a particular science node, security analysis is performed to make sure the addition of the load would not lead to a violation of any voltage or current constraint. If the addition of the load leads to any violation of the system constraints, PMACS will decide the best approach to redistribute the loads at the science nodes. The goal here is to maximize the load to be served according to the

priorities and satisfy all the constraints. Given that the new load is of a particular priority, it is expected to keep all the existing loads with equal or higher priority and shed loads with lower priority during redistribution.

- Receive request from science user
- Check system constraints with additional load
    - Science node voltages
    - Backbone currents
- Determine optimal control actions to be taken if needed
    - Adjust shore station voltages
    - Reduce lower priority loads

4.1.1.2 System Restoration

After a system shutdown, the system restoration procedure is performed in a sequential manner for PMACS to take fault location measurements and the BUs to isolate the backbone/spur cable fault. When the system is restored to normal operating voltage level, there will be a time interval of approximately 4~5 minutes for the NPC and communication devices to restart before PMACS can receive any data or perform any control action to the science nodes. PMACS would then need to perform state estimation and topology identification to identify the new system topology and check if all the operation constraints are satisfied. If not, PMACS would need to calculate to either adjust the shore station voltage output or reduce low priority load at the science node. The algorithm is required to shed the minimum amount of load while maintaining all the constraints.

- Check current system topology
- Check current load profile from all science nodes
- Update power flow algorithm with new topology
- Check system constraints
    - Science node voltages
    - Backbone currents

- Determine best control action to be taken if needed with new topology
    - Adjust shore station voltages
    - Reduce low priority loads

4.1.1.3 On-Line Operation and Control

During operation of the NEPTUNE system, PMACS will monitor all power system data from the shore stations and science nodes. System analysis tools such as State Estimation are performed regularly. If any abnormal condition is detected by PMACS such as voltage violations or over-current problem, the on-line operation and control module will determine the appropriate control actions to be taken to maintain the system in its normal operating state. The control actions can include the adjustment of the shore station voltage or load shedding. The goal is to maximize the total power delivered to the science users while satisfying all the constraints.

- Monitor real time operating state
- Check system constraints
    - Science node voltages
    - Backbone currents
- Determine if any constraint is violated
- Determine optimal control actions to be taken if needed
    - Adjust shore station voltages
    - Reduce lower priority loads

4.2 Nonlinear Optimization Based Load Management

The proposed Load Management module is developed using a nonlinear optimization technique. All loads in the system are categorized according to priority. The Load Management algorithm takes into account the priorities of loads by assigning a weighting factor in the objective function for calculation of the optimal solution as shown in (4.1). The goal of the algorithm is to maximize the amount of power that the system is able to deliver to science users with variable priority while

satisfying all the system constraints including power flow equations, voltage constraints and current constraints.

objective

$$\max \sum_i (w_1 P_{SN_i 1} + w_2 P_{SN_i 2} + w_3 P_{SN_i 3}) \quad i = 1 \cdots m \qquad (4.1)$$

subject to

$$P_{SN_i 1} + P_{SN_i 2} + P_{SN_i 3} = P_{SN_i}$$
$$\underline{P} = V_{Diag} G_{Bus} \underline{V}$$
$$\underline{I}_{BB} \le I_{\max}$$
$$\underline{V}_{SN} \ge V_{Shutdown}$$
$$V_{\min} \le \underline{V}_{SS} \le V_{\max}$$
$$0 \le P_{SN_i 1} \le C_{1i} P_{SN_i Max}$$
$$0 \le P_{SN_i 2} \le C_{2i} P_{SN_i Max}$$
$$0 \le P_{SN_i 3} \le C_{3i} P_{SN_i Max}$$

Where:

m: total number of science nodes

P_{SNi1}, P_{SNi2}, and P_{SNi3}: loads at science node i of each priority

w_1, w_2, and w_3: weighting factors for the loads at each priority

$\underline{P}$: vector of power injections at all the nodes

V_{Diag}: diagonal matrix of the voltages at all the nodes

$\underline{V}$: vector of voltages at all the nodes

G_{Bus}: node conductance matrix

$\underline{I}_{BB}$: vector of the backbone currents.

I_{max}: current limit of the backbone cable.

$\underline{V}_{SN}$: vector of voltages at science nodes

$\underline{V}_{SS}$: vectors of voltages at shore stations

$V_{Shutdown}$: shutdown voltage of the DC-DC converters at the science nodes

V_{min} and V_{max}: minimum and maximum voltage output levels of the shore station power supply

C_{1i}, C_{2i}, and C_{3i}: percentage factors for loads of each priority at science node i

P_{SNiMax}: maximum load at science node i

In the optimization problem defined by (4.1), the objective function is the sum of the total power delivered to all the science nodes in the system. The first constraint assures that the total load at a particular science node equals to the sum of the loads at the three different priorities. The second constraint is the power flow constraint. It means that the operating condition has to satisfy the power flow equations. The third one shows that the backbone current has to be less than or equal to the current limit. The fourth constraint ensures that the science node voltage is higher than the converter shutdown voltage. The fifth constraint shows the range of permissible power supply output voltage. The last three constraints show how the loads at the science node are partitioned into the three different priorities. These percentage factors show how much load is categorized in each priority at a particular science node.

The priorities of the loads at the science nodes are categorized into three levels: high, medium, and low. The weighting factors are constants in the objective function to favor higher priority loads since loads with a higher priority are assigned with a larger weighting factor.

The power injection vector contains power injections at all the nodes including the BU nodes where power injections are zero. The matrix and vector for voltages includes the shore station voltages, science node voltages and branching unit node voltages. The node conductance matrix is similar to the node admittance matrix with only the resistive elements.

The objective of this nonlinear optimization problem is to maximize the total load being served to all science nodes of the system. The problem is solved by Sequential

Quadratic Programming (SQP). While the solution for the optimization problem is continuous, in reality, the science node loads are discrete since they are either connected or disconnected. In order to obtain a meaningful solution for the operator to decide which external loads to be switched on or off, the algorithm needs to produce a discrete solution. The optimal discrete solution to this problem is to choose the closest discrete neighbor of the continuous optimal solution. The solution is obtained by the Branch and Bound technique [42]. This method takes the continuous solution variable and uses the upper and lower discrete neighbor as boundaries for that variable, effectively introducing an integer constraint on the number of loads served. These additional constraints are added to the original set one at a time. After adding the new constraint, the optimization problem is solved again to see whether there is a feasible solution. If there is, then test the other boundary constraint in the same manner. Solutions to the two problems are compared to find the optimal solution of the discrete problem.

4.2.1 Load Management for NEPTUNE

The NEPTUNE system topology is shown in Figure 4.3 with 2 shore stations and 46 science nodes. The cable resistance is assumed to be 1 Ω/km and the cable distances are shown in kilometers.

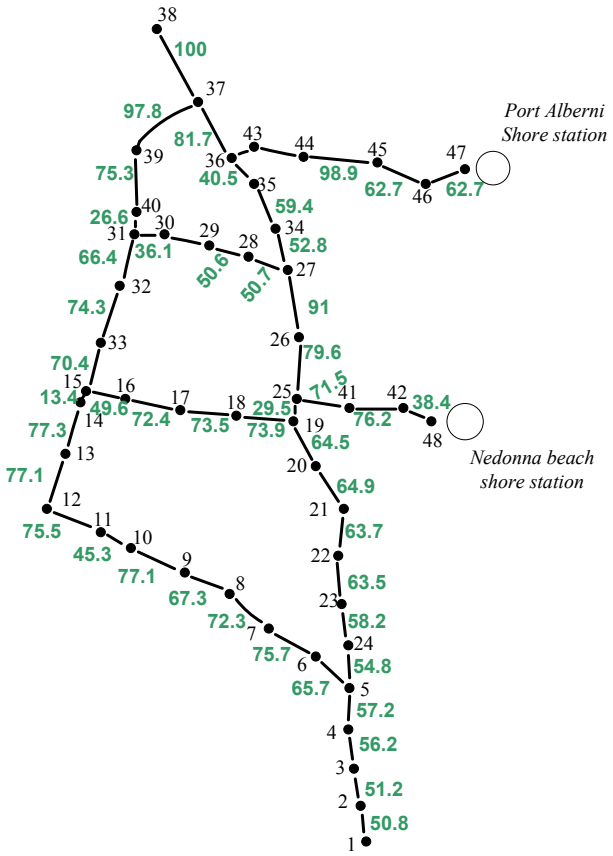

Figure 4.3: NEPTUNE system topology

The internal loads at science nodes are the communications devices. These loads should always be at the highest priority in any situation. The external loads at science nodes are divided into three levels of priority. The priority for a specific science user should be stated in the user contract.

For this system, the variables in (4.1) are defined as the following:

$$\underline{P} = \begin{bmatrix} P_1 \\ \vdots \\ P_{46} \\ P_{47} \\ P_{48} \\ P_{49} \\ \vdots \\ P_{94} \end{bmatrix} = \begin{bmatrix} \underline{P}_{BU} \\ --- \\ \underline{P}_{SS} \\ --- \\ \underline{P}_{SN} \end{bmatrix}$$

$$\underline{P}_{BU} = \begin{bmatrix} P_1 \\ \vdots \\ P_{46} \end{bmatrix} = [0]$$

$$\underline{P}_{SS} = \begin{bmatrix} P_{47} \\ P_{48} \end{bmatrix}$$

$$\underline{P}_{SN} = \begin{bmatrix} P_{SN_1} \\ \vdots \\ P_{SN_{46}} \end{bmatrix} = \begin{bmatrix} P_{49} \\ \vdots \\ P_{94} \end{bmatrix}$$

Where:

$\underline{P}_{BU}$: power injections at the branching unit nodes

$\underline{P}_{SS:}$ power outputs at the shore stations

$\underline{P}_{SN}$: power injections at the science nodes.

$$\underline{V} = \begin{bmatrix} V_1 \\ \vdots \\ V_{46} \\ V_{47} \\ V_{48} \\ V_{49} \\ \vdots \\ V_{94} \end{bmatrix} = \begin{bmatrix} \underline{V}_{BU} \\ --- \\ \underline{V}_{SS} \\ --- \\ \underline{V}_{SN} \end{bmatrix}$$

$$\underline{V}_{BU} = \begin{bmatrix} V_1 \\ \vdots \\ V_{46} \end{bmatrix}$$

$$\underline{V}_{SS} = \begin{bmatrix} V_{47} \\ V_{48} \end{bmatrix}$$

$$\underline{V}_{SN} = \begin{bmatrix} V_{SN_1} \\ \vdots \\ V_{SN_{46}} \end{bmatrix} = \begin{bmatrix} V_{49} \\ \vdots \\ V_{94} \end{bmatrix}$$

$$V_{Diag} = \begin{bmatrix} V_1 & & & 0 \\ & V_2 & & \\ & & \ddots & \\ 0 & & & V_{94} \end{bmatrix}$$

Where:

$\underline{V}_{BU}$: voltages at the branching unit nodes

$\underline{V}_{SS}$: voltage outputs at the shore stations

$\underline{V}_{SN}$: the voltages at the science nodes.

These matrices and vectors are included in the second constraint such that the power flow equations are satisfied. The matrix form of the power flow equations is give by (4.2).

$$\begin{bmatrix} P_1 \\ \vdots \\ P_{94} \end{bmatrix} = \begin{bmatrix} V_1 & & 0 \\ & \ddots & \\ 0 & & V_{94} \end{bmatrix} \begin{bmatrix} G_{1,1} & \cdots & G_{1,94} \\ \vdots & \ddots & \vdots \\ G_{94,1} & \cdots & G_{94,94} \end{bmatrix} \begin{bmatrix} V_1 \\ \vdots \\ V_{94} \end{bmatrix} \qquad (4.2)$$

The third constraint defines maximum allowed current on the backbone cable. Backbone cable current is given by (4.3).

$$\underline{I}_{BB} = \begin{bmatrix} I_{BB1} \\ \vdots \\ I_{BB50} \end{bmatrix} = \left(AG_{BB}\right)^T \begin{bmatrix} \underline{V}_{BU} \\ \underline{V}_{SS} \end{bmatrix} \tag{4.3}$$

Where:

A: node incidence matrix

G_{BB}: backbone cable conductance matrix.

Table III shows a list of the system parameters and their limits.

Table III: System parameter limits

Name of Parameter	**Symbol**	**Value (unit)**
Backbone Current Limit	I_{max}	10 A
Converter Shutdown Voltage	$V_{shutdown}$	5.9 kV
Shore Station Maximum Voltage Output	V_{max}	11 kV
Shore Station Minimum Voltage Output	V_{min}	9 kV

In the following section, the 48 node system is used as a test case to show the results of the proposed load management algorithm for different scenarios.

4.3 Test Scenarios and Numerical Results

The test scenarios in this sections are based on the system topology shown in Figure 4.2 and the parameters defined in Table III.

4.3.1 Scenario 1

The internal load is assumed to be 1000 W. The efficiency of the DC-DC converters is assumed to be 93 %. For the external load, loads at the high priority are assumed to be up to 1000 W at each science node. Loads with medium and low priorities are assumed to be up to 4000 W and 4000 W respectively. The increment of the loads is assumed to be 50 W. The voltage outputs at the two power supplies are fixed at 10 kV. The solution is shown in Table IV. Although the system has 48 nodes in total, the 2 shore stations do not serve underwater loads. Hence, only 46 underwater nodes are serving science users.

In this scenario, the first 2000 W at each science node is used to serve the internal loads and high priority loads. The remaining power at each science node is used to serve the medium priority loads and no low priority load is served. Notice that this scenario shows the optimal operating condition of the system under which the maximum amount of power is served without any load scheduling. The total power being delivered to the science nodes is 122.4 kW. The total power input from the shore stations is 152.7 kW. The difference represents losses of the converters and cables

Table IV: Optimal solution for 48 node system

Node #	Power (W)	**Node #**	Power (W)	**Node #**	Power (W)
1	2700	**17**	2700	**33**	2650
2	2700	**18**	2700	**34**	2650
3	2700	**19**	2700	**35**	2650
4	2700	**20**	2700	**36**	2700
5	2700	**21**	2700	**37**	2700
6	2650	**22**	2700	**38**	2700
7	2650	**23**	2700	**39**	2650
8	2650	**24**	2700	**40**	2650
9	2650	**25**	2700	**41**	2650
10	2650	**26**	2650	**42**	2650
11	2650	**27**	2650	**43**	2650
12	2600	**28**	2600	**44**	2650
13	2600	**29**	2600	**45**	2650
14	2600	**30**	2600	**46**	2650
15	2600	**31**	2600		
16	2700	**32**	2650		

4.3.2 Scenario 2

In this scenario, it is assumed that the operating condition is the following: 1000 W of internal load, 500 W of high priority load, 700 W of medium priority, and 300 W of low priority at each science node. The high priority science users at each science node request to turn on 200 W at every science node. A power flow simulation of the system shows that there will be a violation of the current constraints by adding the new loads without disconnecting any existing loads. Therefore, some lower priority loads have to be shed. By applying the proposed optimization algorithm with the

additional loads as new constraints, a new operating condition can be obtained by shedding some lower priority loads at science nodes to satisfy the system constraints. The result is shown in Table V.

Table V: Solution for scenario 2

Node #	Power (W)	**Node #**	Power (W)	**Node #**	Power (W)
1	2500	**17**	2600	**33**	2500
2	2500	**18**	2600	**34**	2600
3	2500	**19**	2650	**35**	2600
4	2600	**20**	2700	**36**	2700
5	2600	**21**	2700	**37**	2700
6	2600	**22**	2700	**38**	2700
7	2600	**23**	2700	**39**	2700
8	2600	**24**	2700	**40**	2700
9	2600	**25**	2700	**41**	2600
10	2600	**26**	2600	**42**	2600
11	2600	**27**	2600	**43**	2600
12	2550	**28**	2500	**44**	2600
13	2550	**29**	2500	**45**	2600
14	2550	**30**	2500	**46**	2600
15	2500	**31**	2500		
16	2600	**32**	2500		

In this case, some of the low priority loads at a number of science nodes need to be shed in order for the high priority loads to be switched on while satisfying the system constraints. The actual load switching procedure will be performed by an operator based on the terms described in the user contract. A sample of the proposed user contract is included in the Section 4.4.

4.3.3 Scenario 3

In the case of a backbone cable fault, the NEPTUNE power system will completely shut down to prevent damages due to the high fault current. The system will then perform fault location and isolation at a much lower voltage level (≈ 500 V) to isolate the faulted link so that the rest of the system can be restored. After the process is complete, the system is restored back to the normal operating voltage. Since the post-fault system topology has changed, it is likely that the system cannot supply power at its optimal level. The Load Management algorithm is used to decide the best operating condition and appropriate actions to take.

In this scenario, suppose the link connecting node 46 and 47 has experienced a backbone cable fault and is isolated. Effectively the Port Alberni shore station is out of service. The system would not be able to operate at the pre-fault operating condition in the new topology since only the Nedonna Beach shore station is able to supply power. An optimal solution for this new topology is obtained by the optimization algorithm and the results are shown in Table VI.

The result shows that only about 60 % of the original load can be served if the Port Alberni shore station is out of service; therefore, loads with lower priorities will be switched off in order to satisfy the system constraints

Table VI: Solution for scenario 3

Node #	Power (W)	**Node #**	Power (W)	**Node #**	Power (W)
1	1500	**17**	1500	**33**	1450
2	1500	**18**	1500	**34**	1450
3	1500	**19**	1500	**35**	1450
4	1500	**20**	1500	**36**	1450
5	1500	**21**	1500	**37**	1450
6	1450	**22**	1500	**38**	1450
7	1450	**23**	1500	**39**	1450
8	1450	**24**	1500	**40**	1450
9	1450	**25**	1500	**41**	1500
10	1450	**26**	1450	**42**	1500
11	1450	**27**	1450	**43**	1450
12	1450	**28**	1450	**44**	1450
13	1450	**29**	1450	**45**	1450
14	1450	**30**	1450	**46**	1450
15	1500	**31**	1450		
16	1500	**32**	1450		

4.4 NEPTUNE Power System User Contract

The user contract is the agreement between the science users and NEPTUNE. The information in the contract should contain the priority and type of the load, precise time schedule of the load, and detail sensor network infrastructure. A simplified version sample user contract is included in Section 4.4.1.

4.4.1 Sample User Contract

NEPTUNE Power hereby agrees to supply electrical service to Science User and to permit the User to consume power for the loads listed on Appendix A per the prescribed schedule, attached hereto and as may be hereinafter amended.

NEPTUNE Power desires to set forth the terms and conditions under which power will be supplied to the User under the schedule selected. Three schedules of power delivery will be available for the customer to choose between, schedule A, schedule B, and schedule C. The three schedules of power represent a priority of supply.

Schedule A Power: This represents the highest priority of supply. Loads under schedule A will be the last science loads de-energized in the event of system overloading.

Schedule B Power: This represents the mid range priority of supply. Loads under schedule B de-energized before schedule A loads but after schedule C loads in the event of system overloading.

Schedule C Power: This represents the lowest priority of supply. Loads under schedule C will be the first science loads de-energized in the event of system overloading.

Power will be supplied under the following conditions:

1. User understands and agrees that electric service under all three schedules may be interrupted by NEPTUNE Power at any time that a system emergency exists and load reduction is needed to maintain system integrity.

2. User understands that load shedding will be performed in accordance with the load schedules but that system integrity supersedes the load schedule hierarchy.

3. Changes in user load due to trigger events or environmental changes must be fully documented in Appendix A. Incorrect documentation of load characteristics may result in the load being disconnected from the NEPTUNE infrastructure, both power and communications.

Appendix A:

Load 1 Profile:

1) Load description:
2) Peak load:
3) Load type:
4) Duty cycle:
5) Trigger events:

a. load energized by trigger event:
b. load de-energized by trigger event:

6) Load schedule:

4.5 Summary

In this chapter, an optimization based load management algorithm is presented for NEPTUNE. The approach is to maximize the total load taking into account the system constraints as well as load priorities. Although the nonlinear optimization approach only solves the problem with continuous variables, a discrete solution is obtained by selecting the closest neighbor of the continuous solution.

The Observatory Control System (OCS) that has access to all the PMACS and Data Communication System (DCS) functionalities will serve as the high level control for NEPTUNE. The user contract aspects described in this paper will be handled by the OCS, likely with a significant degree of autonomy.

Chapter 5: Optimization Based Method to Identify Cable Resistance

In terrestrial power systems, parameter identification and system modeling are normally performed to identify and update system models for dynamic simulation [23] – [28]. Such studies are needed due to the fact that accurate models are required in order to perform stability analysis. An inaccurate model may fail to predict the outcome of a system disturbance or operation, resulting in an unexpected or undesired system state.

5.1 Parameter Identification for NEPTUNE

One of the essential data categories acquired by the NEPTUNE PMACS is the system topology with node connections and cable resistances. All the PMACS functions including State Estimation, Fault Location, and Load Management require this knowledge to produce an accurate result. Therefore, the system model used in these modules needs to be as accurate as possible.

The cable resistances being used in the system models of the PMACS EMS modules are assumed to be constant based on resistance per unit length and cable length. The cable length does not change but the resistance per unit length is not a constant due to the temperature of seawater. Since the size of the overall system contains over a few thousand kilometers of cable, a small change in the resistance per unit length could lead to a significant error especially for functions that require accurate data. In the case of State Estimation, the voltages at the branching unit nodes and currents on the backbone cables are not directly measured but estimated based on the available measurements from the shore stations and science nodes. The estimation algorithm described in [37] uses the assumed cable resistances in the model. If the

value used in the model is not a good representation of the actual system, the estimated outcomes may provide false information. In Load Management, the algorithm uses the system model in the process to constraint the science node voltages and backbone currents to make sure the system stays within normal operating conditions before a science node load is turned on or off. An error in the cable resistance may result in a violation of voltage or current limit. The Fault Location module of PMACS requires accurate knowledge of the cable resistance since the estimation of the location of the fault is based on only the measurements from the shore stations and the network topology. The outcome from this module can not provide an accurate result if the system topology model is not accurate. As a result, PMACS needs to be able to adjust the cable resistances in the models for the module to provide the desired functionality.

5.2 Cable Resistance Variation

Cable resistances are normally specified at a particular temperature. The actual resistance of the cable varies with respect to the temperature with a temperature coefficient. A typical temperature coefficient for submarine cables is about 0.4 %/°C. For example, the cable resistance for TyCom SL-21 cable is 0.73 Ω/km at 3 °C and 0.78 Ω/km at 20 °C. In the same manner, several degrees of temperature difference of the seawater can lead to a change of a few percent in the cable resistance. The actual cable resistance per unit length can be calculated based on (5.1).

$$R_A = R_S + R_S(T_A - T_S)\alpha \qquad (5.1)$$

Where:

R_A: actual resistance per unit length

R_S: manufacture specified resistance per unit length at a specific temperature

T_A: actual temperature in °C

T_S: manufacture specified temperature

α: temperature coefficient in %/°C.

Seawater temperature varies seasonally and cable sections close to the shore are likely to experience a larger variation in terms of temperature. From historical data of ocean bottom temperature in [43] – [44], it can be seen that the temperature varied over a range of approximately 1 °C to 7 °C depending on the location of the measurements. This observation shows that the cable resistances in this area can vary over a range of approximately 3 %. If the cable resistance is specified at 1 Ω/km and the section is 100 km long, the actual cable resistance a cable section is 103 Ω while the modeled resistance is only 100 Ω. If the current on this is 5 A, the difference in voltage drop is 15 V. For NEPTUNE, temperature compensation for cable resistance needs to be taken into account due to the physical size of the system. The total length of cables used in NEPTUNE is over a thousand kilometers.

5.3 Optimization Based Cable Resistance Identification

For the NEPTUNE system, the loads at the science nodes are controlled by PMACS. At any given time under a normal operating condition, PMACS has information on the amount of power being delivered to each science node. The voltage outputs at the shore stations are collected by the Power Supply Controller and sent to the PMACS Console by the Server every second. PMACS can perform power flow analysis of the system using (5.2).

$$P_i = V_i \sum_{1}^{n} Y_{ik} V_k \qquad (5.2)$$

Where:

n: number of nodes

P_i: power injection at node i

V_i, V_k: node voltages at nodes i and k respectively

Y_{ik}: element of the node admittance matrix

The power injection at a specific bus is defined to be the power being injected into the system. For a bus with a generator connected to the transmission system this value will simply be the output power of the generator, since generators will inject power into the transmission system. For a load bus it will be the negative of the load since loads will remove power from the transmission system. For busses with both a generator and loads, the injection will be the net sum of the two values. For the NEPTUNE power system the generators are the two shore stations which have no scientific loads. The loads are the science users at the science nodes, which have no generators. Since NEPTUNE is a DC system, the node admittance matrix can be simplified to the node conductance matrix which contains only the real-valued element as in (5.3). In this case, the off-diagonal elements, G_{ik}, of the node conductance matrix are the negative values of the reciprocal of the cable resistances connecting nodes i and k. The diagonal elements, G_{ii}, are the sum of all the reciprocal of the cable resistances connected to node i. The solution to this power flow problem is the voltages at the load busses and power outputs at the generator busses which can be solved by various numerical methods.

$$P_i = V_i \sum_{1}^{n} G_{ik} V_k \qquad (5.3)$$

Where:

G_{ik}: conductance between nodes i and k

The real-time voltage measurements at the science nodes are collected by the Node Power Controller and the data is sent to the PMACS Console from the Server once every second. The power output, voltage and current outputs at both shore stations are also collected by the Shore Power Controller. These measurements are also sent to the Console from the Server every second. For the purpose of this study, the voltages measured at the science nodes are used as input parameters into the power flow formulation to calculate the resulting power injection at the nodes. Once the power flow problem is solved and solutions obtained, these values are compared with the real-time measurements to check if they match each other. If the values are matched, it means that the model used in the power flow formulation is correct; otherwise, the model needs to be updated to reflect the actual system condition. To update the model of the system, the cable resistances need to be adjusted.

5.3.1 Quadratic Programming for Resistance Update

Since the errors between the measured and calculated power injections at the nodes can be positive or negative, linear optimization technique cannot be used to solve this problem and hence, in order to update the cable resistance, the quadratic programming technique is used to minimize the sum of the squares of the errors. The general form of quadratic programming is shown in (5.4).

$$\min_{x} \frac{1}{2} x^T H x + f^T x \qquad (5.4)$$

Subject to:

$$Ax \le b$$
$$A_{eq} x = b_{eq}$$
$$lb \le x \le ub$$

Which:

H: (n x n) symmetric matrix describing the coefficients of the quadratic terms

f: n-dimensional column vector describing the coefficients of the linear terms

A, b: inequality constraints

A_{eq}, b_{eq}: equality constraints

lb, *ub*: lower bound and upper bound for the decision variables

x: column vector of decision variables

In this study, the decision variables will be the elements of the node conductance matrix, G_{ik}, and the H matrix and f vector are elements consist of the node power injections and voltages. To put the problem into the general form of a quadratic programming problem as in (5.4), start by rewriting (5.3) for all n busses into (5.5) and (5.6).

$$P_1 = V_1^2 G_{1,1} + V_1 V_2 G_{1,2} + \cdots + V_1 V_n G_{1,n} \tag{5.5}$$

$$\vdots$$

$$P_n = V_n V_1 G_{n,1} + \cdots + V_n V_{n-1} G_{n,n-1} + V_n^2 G_{n,n} \tag{5.6}$$

The *n* equations can be expressed in a matrix form (5.7).

$$\underline{P} = V_{Diag} G_{Bus} \underline{V} \tag{5.7}$$

Where:

$$\underline{P} = \begin{bmatrix} P_1 \\ \vdots \\ P_n \end{bmatrix}$$

$$V_{Diag} = \begin{bmatrix} V_1 & & 0 \\ & \ddots & \\ 0 & & V_n \end{bmatrix}$$

$$G_{Bus} = \begin{bmatrix} G_{1,1} & \cdots & G_{1,n} \\ \vdots & \ddots & \vdots \\ G_{n,1} & \cdots & G_{n,n} \end{bmatrix}$$

$$\underline{V} = \begin{bmatrix} V_1 \\ \vdots \\ V_n \end{bmatrix}$$

Since the G_{Bus} matrix is symmetric, only the diagonal elements and the off-diagonal elements in either the upper or lower triangle are needed. These elements are the entries of vector $\underline{G}$.

$$\underline{G} = \begin{bmatrix} G_{1,1} \\ G_{1,2} \\ \vdots \\ G_{n-1,n} \\ G_{n,n} \end{bmatrix} = \begin{bmatrix} G_1 \\ G_2 \\ \vdots \\ G_{\frac{(1+n)n}{2}-1} \\ G_{\frac{(1+n)n}{2}} \end{bmatrix}$$

The mth element of this vector, G_m, is the element G_{ik} in the G_{Bus} matrix with the following condition (5.8).

$$m = (i-1)n + k - \frac{(i-1)i}{2} \qquad (5.8)$$

By rearranging (5.7), it can be expressed as (5.9).

$$\underline{P} = V_{matrix}\underline{G} \tag{5.9}$$

Where:

V_{matrix}: $n \times \frac{(1+n)n}{2}$ matrix with entries as in (5.10)

$$V_{matrix}(j,m) = \begin{cases} V_i V_k & \text{if } G_m = G_{ik} \neq 0 \text{ and } j = i \text{ or } k \\ 0 & \text{otherwise} \end{cases} \tag{5.10}$$

The error between the measured and calculated power injection at node i is given by (5.11).

$$\varepsilon_i = P_i - \left(V_i \sum_{k=1}^{n} G_{ik} V_k \right) \tag{5.11}$$

Where:

ε_i: error of power injection at node i

The square of the error is given by (5.12).

$$\begin{aligned} \varepsilon_i^2 &= \left[P_i - \left(V_i \sum_{k=1}^{n} G_{ik} V_k \right) \right]^2 \\ &= P_i^2 - 2P_i \left(V_i \sum_{k=1}^{n} G_{ik} V_k \right) + \left(V_i \sum_{k=1}^{n} G_{ik} V_k \right)^2 \end{aligned} \tag{5.12}$$

For a specific node i, assuming node i is connected to nodes j, k, and l, the equations (5.5), (5.11), and (5.12) can be written as (5.13), (5.14), and (5.16).

$$P_i = V_i^2 G_{i,i} + V_i V_j G_{i,j} + V_i V_k G_{i,k} + V_i V_l G_{i,l} \tag{5.13}$$

$$\begin{aligned}\varepsilon_i &= P_i - \left(V_i^2 G_{i,i} + V_i V_j G_{i,j} + V_i V_k G_{i,k} + V_i V_l G_{i,l}\right) \\ &= P_i - V_i^2 G_{i,i} - V_i V_j G_{i,j} - V_i V_k G_{i,k} - V_i V_l G_{i,l}\end{aligned} \tag{5.14}$$

$$\begin{aligned}\varepsilon_i^2 &= V_i^4 G_{i,i}^2 + V_i^2 V_j^2 G_{i,j}^2 + V_i^2 V_k^2 G_{i,k}^2 + V_i^2 V_l^2 G_{i,l}^2 \\ &\quad + 2V_i^3 V_j G_{i,i} G_{i,j} + 2V_i^3 V_k G_{i,i} G_{i,k} + \cdots \\ &\quad - 2P_i V_i^2 G_{i,i} - \cdots + P_i^2\end{aligned} \tag{5.15}$$

The sum of the square of the errors, ε_T, is given by (5.16).

$$\varepsilon_T = \sum_{i=1}^{n} \varepsilon_i^2 \tag{5.16}$$

The matrix form of (5.16) can be obtained by substituting (5.9) and (5.12) into (5.16) as in (5.16).

$$\begin{aligned}\varepsilon_T &= \underline{G}^T A \underline{G} + B^T \underline{G} + \underline{P}^T \underline{P} \\ &= \begin{bmatrix} G_{1,1} \\ G_{1,2} \\ \vdots \\ G_{n-1,n} \\ G_{n,n} \end{bmatrix}^T A \begin{bmatrix} G_{1,1} \\ G_{1,2} \\ \vdots \\ G_{n-1,n} \\ G_{n,n} \end{bmatrix} + B^T \begin{bmatrix} G_{1,1} \\ G_{1,2} \\ \vdots \\ G_{n-1,n} \\ G_{n,n} \end{bmatrix} + \begin{bmatrix} P_1 \\ \vdots \\ P_n \end{bmatrix}^T \begin{bmatrix} P_1 \\ \vdots \\ P_n \end{bmatrix}\end{aligned} \tag{5.17}$$

Where:

$$A_{ij} = \sum_{u=1}^{n} V_{matrix}(u,i) \times V_{matrix}(u,j) \qquad i,j = 1,\cdots,\frac{(1+n)n}{2}$$

$$B_m = -2\sum_{i=1}^{n} P_i V_{matrix}(i,m)$$

(5.17) is consistent with the general form of quadratic programming problem as shown in (5.4). Since a constant term does not affect the outcome of an optimization problem, the last term in (5.17) can be dropped from the model. By multiplying all of the entries of the matrix A by 2, (5.17) becomes the general form of the quadratic programming and can be solved using MATLAB. The function evaluated at the solution is compared to the sum of all power injections at the nodes to ensure that the algorithm provides an acceptable solution. To illustrate the procedure of problem formulation and the construction of the matrices and vectors, a simple 4-bus system is shown in the Section 5.3.2.

5.3.2 Four Bus System Test Case

A 4-bus simple system as shown in Figure 5.1 is used to show the formulation of the quadratic programming algorithm as described in the last section.

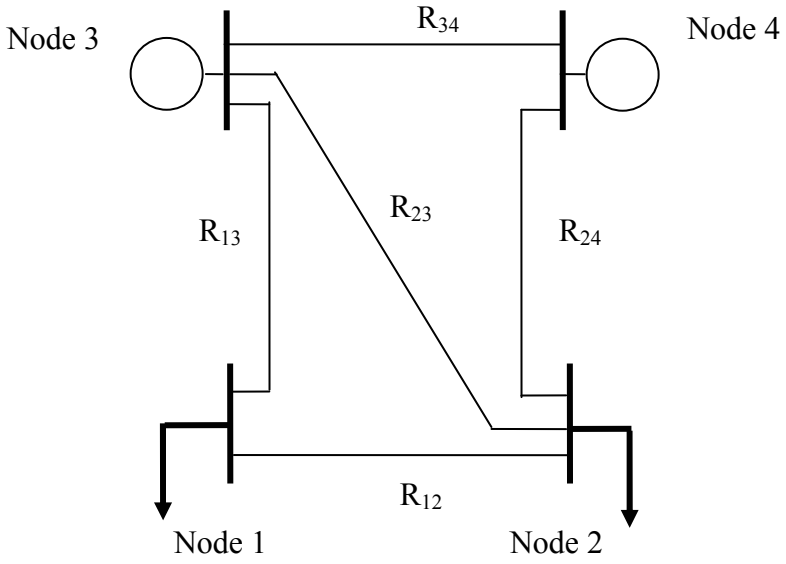

Figure 5.1: 4-bus system

$R_{12} = 250\ \Omega$ $R_{13} = 250\ \Omega$ $R_{23} = 300\ \Omega$ $R_{24} = 200\ \Omega$ $R_{34} = 200\ \Omega$

The loads at nodes 1 and 2 are both 2000 W; therefore, the power injections P_1 and P_2 are both equal to -2000 W. The generators are located at nodes 3 and 4, the voltage outputs at these 2 nodes are assumed to be fixed at 10000V. The node conductance matrix for this system is:

$$G_{Bus} = \begin{bmatrix} 0.008 & -0.004 & -0.004 & 0 \\ -0.004 & 0.01233 & -0.0033 & -0.005 \\ -0.004 & -0.0033 & 0.01233 & -0.005 \\ 0 & -0.005 & -0.005 & 0.01 \end{bmatrix}$$

The power flow solution of this system gives the following results:

$P_3 = 2557.4$ W $P_4 = 1456.4$ W

$V_1 = 9960.33$ V $V_2 = 9970.87$ V

The matrix representation of (5.7) and (5.9) for this system are given by:

$$\begin{bmatrix} P_1 \\ P_2 \\ P_3 \\ P_4 \end{bmatrix} = \begin{bmatrix} V_1 & 0 & 0 & 0 \\ 0 & V_2 & 0 & 0 \\ 0 & 0 & V_3 & 0 \\ 0 & 0 & 0 & V_4 \end{bmatrix} G_{Bus} \begin{bmatrix} V_1 \\ V_2 \\ V_3 \\ V_4 \end{bmatrix}$$

$$\begin{bmatrix} P_1 \\ P_2 \\ P_3 \\ P_4 \end{bmatrix} = \underbrace{\begin{bmatrix} V_{11}^2 & V_1V_2 & V_1V_3 & 0 & 0 & 0 & 0 & 0 & 0 & 0 \\ 0 & V_1V_2 & 0 & 0 & V_2^2 & V_2V_3 & V_2V_4 & 0 & 0 & 0 \\ 0 & 0 & V_1V & 0 & 0 & V_2V_3 & 0 & V_3^2 & V_3V_4 & 0 \\ 0 & 0 & 0 & 0 & 0 & 0 & V_2V_4 & 0 & V_3V_4 & V_4^2 \end{bmatrix}}_{V_{matrix}} \underbrace{\begin{bmatrix} G_{11} \\ G_{12} \\ G_{13} \\ G_{14} \\ G_{22} \\ G_{23} \\ G_{24} \\ G_{33} \\ G_{34} \\ G_{44} \end{bmatrix}}_{\underline{G}}$$

Since G_{14} is zero in this system, V_{matrix} and $\underline{G}$ can be reduced by omitting the corresponding column and row. Following the formulation described in the last section, the resulting matrix A, vector B and the total squared error, ε_T, are given by:

$$\varepsilon_T = \begin{bmatrix} G_{11} \\ \vdots \\ G_{44} \end{bmatrix}^T A \begin{bmatrix} G_{11} \\ \vdots \\ G_{44} \end{bmatrix} + B^T \begin{bmatrix} G_{11} \\ \vdots \\ G_{44} \end{bmatrix} + \begin{bmatrix} P_1 \\ \vdots \\ P_4 \end{bmatrix}^T \begin{bmatrix} P_1 \\ \vdots \\ P_4 \end{bmatrix}$$

$$A = \begin{bmatrix} V_1^4 & V_1^3V_2 & V_1^3V_3 & 0 & 0 & 0 & 0 & 0 & 0 \\ V_1^3V_2 & 2V_1^2V_2^2 & V_1^2V_2V_3 & V_1V_2^3 & V_1V_2^2V_3 & V_1V_2^2V_4 & 0 & 0 & 0 \\ V_1^3V_3 & V_1^2V_2V_3 & 2V_1^2V_3^2 & 0 & V_1V_2V_3^2 & 0 & V_1V_3^3 & V_1V_3^2V_4 & 0 \\ 0 & V_1V_2^3 & 0 & V_2^4 & V_2^3V_3 & V_2^3V_4 & 0 & 0 & 0 \\ 0 & V_1V_2^2V_3 & V_1V_2V_3^2 & V_2^3V_3 & 2V_2^2V_3^2 & V_2^2V_3V_4 & V_2V_3^3 & V_2V_3^2V_4 & 0 \\ 0 & V_1V_2^2V_4 & V_1V_2V_3^2 & V_2^3V_4 & V_2^2V_3V_4 & 2V_2^2V_4^2 & 0 & V_2V_3V_4^2 & V_2V_4^3 \\ 0 & 0 & V_1V_3^3 & 0 & V_2V_3^3 & 0 & V_3^4 & V_3^3V_4 & 0 \\ 0 & 0 & V_1V_3^2V_4 & 0 & V_2V_3^2V_4 & V_2V_3V_4^2 & V_3^3V_4 & 2V_3^2V_4^2 & V_3V_4^3 \\ 0 & 0 & 0 & 0 & 0 & V_2V_4^3 & 0 & V_3V_4^3 & V_4^4 \end{bmatrix}$$

$$B = \begin{bmatrix} -2P_1V_1^2 \\ -2P_1V_1V_2 - 2P_2V_1V_2 \\ -2P_1V_1V_3 - 2P_3V_1V_3 \\ -2P_2V_2^2 \\ -2P_2V_2V_3 - 2P_3V_2V_3 \\ -2P_2V_2V_4 - 2P_4V_2V_4 \\ -2P_3V_3^2 \\ -2P_3V_3V_4 - 2P_4V_3V_4 \\ -2P_4V_4^2 \end{bmatrix}$$

These parameters are used as inputs to the quadratic programming algorithm described in (5.4) and it becomes:

$$\min_G \frac{1}{2} \begin{bmatrix} G_{11} \\ G_{12} \\ G_{13} \\ G_{22} \\ G_{23} \\ G_{24} \\ G_{33} \\ G_{34} \\ G_{44} \end{bmatrix}^T \begin{bmatrix} 2V_1^4 & 2V_1^3V_2 & 2V_1^3V_3 & 0 & 0 & 0 & 0 & 0 & 0 \\ 2V_1^3V_2 & 4V_1^2V_2^2 & 2V_1^2V_2V_3 & 2V_1V_2^3 & 2V_1V_2^2V_3 & 2V_1V_2^2V_4 & 0 & 0 & 0 \\ 2V_1^3V_3 & 2V_1^2V_2V_3 & 4V_1^2V_3^2 & 0 & 2V_1V_2V_3^2 & 0 & 2V_1V_3^3 & 2V_1V_3^2V_4 & 0 \\ 0 & 2V_1V_2^3 & 0 & 2V_2^4 & 2V_2^3V_3 & 2V_2^3V_4 & 0 & 0 & 0 \\ 0 & 2V_1V_2^2V_3 & 2V_1V_2V_3^2 & 2V_2^3V_3 & 4V_2^2V_3^2 & 2V_2^2V_3V_4 & 2V_2V_3^3 & 2V_2V_3^2V_4 & 0 \\ 0 & 2V_1V_2^2V_4 & 2V_1V_2V_3^2 & 2V_2^3V_4 & 2V_2^2V_3V_4 & 4V_2^2V_4^2 & 0 & 2V_2V_3V_4^2 & 2V_2V_4^3 \\ 0 & 0 & 2V_1V_3^3 & 0 & 2V_2V_3^3 & 0 & 2V_3^4 & 2V_3^3V_4 & 0 \\ 0 & 0 & 2V_1V_3^2V_4 & 0 & 2V_2V_3^2V_4 & 2V_2V_3V_4^2 & 2V_3^3V_4 & 4V_3^2V_4^2 & 2V_3V_4^3 \\ 0 & 0 & 0 & 0 & 0 & 2V_2V_4^3 & 0 & 2V_3V_4^3 & 4V_4^4 \end{bmatrix} \begin{bmatrix} G_{11} \\ G_{12} \\ G_{13} \\ G_{22} \\ G_{23} \\ G_{24} \\ G_{33} \\ G_{34} \\ G_{44} \end{bmatrix}$$

$$+ \begin{bmatrix} -2P_1V_1^2 \\ -2P_1V_1V_2 - 2P_2V_1V_2 \\ -2P_1V_1V_3 - 2P_3V_1V_3 \\ -2P_2V_2^2 \\ -2P_2V_2V_3 - 2P_3V_2V_3 \\ -2P_2V_2V_4 - 2P_4V_2V_4 \\ -2P_3V_3^2 \\ -2P_3V_3V_4 - 2P_4V_3V_4 \\ -2P_4V_4^2 \end{bmatrix}^T \begin{bmatrix} G_{11} \\ G_{12} \\ G_{13} \\ G_{22} \\ G_{23} \\ G_{24} \\ G_{33} \\ G_{34} \\ G_{44} \end{bmatrix}$$

The constant term which is the sum of the squares of all power injections at the nodes is dropped from the formulation. Since we know the diagonal elements of the G_{Bus} matrix are positive and the off-diagonal elements are negative, these are used as the inequality constraints. For the equality constraints, the diagonal elements of the G_{Bus} matrix, G_{ii}, is the sum of all conductance connected to node i. The upper bound and lower bound of the decision variables are set at ± 2 % of the cable resistance.

Assuming the actual cable resistances are 2 % smaller than the known values, a power flow analysis is performed to generate voltage outputs at the nodes. These voltages are used as the measured voltages at the science nodes. Feeding these values back into the original model produces a mismatch in terms of power injections at the nodes. The quadratic programming algorithm is then used to solve for a new set of conductance that would minimize the total squared error by MATLAB. The results are shown in Table VII.

Table VII: Simulation results for the 4-bus system

	Actual Cable Resistance (Ω)	**Estimated cable Resistance (Ω)**
$\mathbf{R_{12}}$	245	245.1
$\mathbf{R_{13}}$	245	245.0
$\mathbf{R_{23}}$	294	293.8
$\mathbf{R_{24}}$	196	196.1
$\mathbf{R_{34}}$	196	196.2

5.3.3 Validation of the Resistance Identification Algorithm

For a quadratic programming problem, a sufficient condition for a unique global solution is that the matrix H in (5.4) is positive definite. However, the matrix H in the

NEPTUNE problem is not positive definite. Therefore, a global optimal solution can not be guaranteed.

Since the decision variables in this problem are the resistances of the backbone cables, it is not likely to vary over a large range but a smaller range within a few percent. The actual percentage can be determined by historical data of the ocean temperature in the area. If real-time temperature is available, the constraints in the formulation can be adjusted to reflect the appropriate values.

Once a solution is obtained from the algorithm, the function evaluation of (5.4) is compared to the sum of all power injections at the nodes. If the difference between the two is small enough, the solution correctly updates the system model to reflect the change of parameters.

5.4 Simulation Results for the NEPTUNE System

The 48-bus system shown in Figure 4.2 is used to test the resistance identification module described in the chapter. The length of the backbone cables is in kilometers while the resistance of the cable is assumed to be 1 Ω/km. The length of all the spur cables is assumed to be 5km. The temperature coefficient of the cables is assumed to be 0.4 %/°C. The first step is to construct V_{matrix} and $\underline{G}$ in (5.9). There are a total of 94 nodes with 46 science nodes, 46 branching unit nodes, and 2 shore stations. The total number of cable sections is 96 with 50 backbone cables connecting the branching unit nodes and shore stations and 46 spur cables connecting the branching unit nodes and the science nodes. The dimensions of V_{matrix} and $\underline{G}$ are 94×4656 and 4656×1 respectively. However, due to the sparse nature of the G_{Bus} matrix, most of the non-diagonal elements are zero. The actual dimensions are 94×190 and 190×1 instead. The dimensions of A and B are therefore 190×190 and 190×1. The construction of these matrices and vectors are described in the Chapter 5.3.1.

5.4.1 Test Case 1

Assuming the ocean bottom temperature has changed by +5 °C, this change in temperature will lead to a resistance increase by approximately 2 %. Since the spur cable is short and the change in resistance is insignificant, only the resistances of the backbone cables are changed. A power flow analysis is performed to simulate the measured voltages at the science nodes. These voltages are inputted into (5.7) with the original G_{Bus} model. Due to the inconsistency between the power flow model and the actual system parameter, the resulting power injections at the science nodes do not match the values observed by PMACS. Then resistance identification module is performed to a new set of backbone cable resistance with the objective to minimize the mismatch between the power flow outputs and observed values. The results are shown in Table VIII.

From the results shown in Table VIII, it can be seen that the optimization based resistance identification algorithm is able to update the resistance of the model to reflect the real world scenario. The new model is a better representation of the system.

Table VIII: Estimated resistance for test case 1

Link #	R(Ω)	Estimated R(Ω)	Link #	R(Ω)	Estimated R(Ω)	Link #	R(Ω)	Estimated R(Ω)
1	102	101.5	**18**	68.65	68.22	**35**	63.95	63.93
2	83.3	82.88	**19**	78.64	78.3	**36**	72.93	72.89
3	41.31	41.3	**20**	46.21	45.89	**37**	77.72	77.7
4	60.59	60.18	**21**	77.01	76.31	**38**	19.17	19.16
5	53.86	53.8	**22**	78.64	78.05	**39**	58.34	58.02
6	92.82	92.26	**23**	78.85	78.1	**40**	57.32	56.95
7	81.19	81.06	**24**	13.67	13.56	**41**	52.22	51.14
8	30.09	29.73	**25**	71.81	71.44	**42**	51.82	51.25
9	65.79	65.2	**26**	74.46	74.08	**43**	36.82	36.4
10	66.2	65.95	**27**	65.28	64.86	**44**	57.53	57.28
11	64.97	64.58	**28**	27.13	27.01	**45**	51.61	51.26
12	64.77	64.28	**29**	76.81	76.38	**46**	51.71	51.28
13	59.36	58.99	**30**	99.76	99.14	**47**	50.59	49.98
14	55.9	55.1	**31**	30.09	29.8	**48**	73.85	73.31
15	67.01	66.52	**32**	70.18	69.88	**49**	74.97	74.29
16	77.21	76.82	**33**	100.88	100.8	**50**	75.38	74.66
17	73.75	73.41	**34**	63.95	63.92			

5.4.2 Test Case 2

In this test case, it is assumed that the temperature has been increased by 10 °C which can lead to a change in resistance of up to 4 %. However, the constraints in the optimization formulation only allow the resistance to change over the range of 2 %. In this case, the updated resistance values reach the limits and conclude that is the best solution within the feasible region. The results are shown in Table IX.

As shown in Table IX, the updated resistances do not provide a significant improvement since the range of resistance variation is too large. However, the performance can be improved if the constraints in the algorithm are updated to allow a higher limit. For example, if real-time seawater temperature is available to PMACS,

the module can adjust the constraints in the algorithm to compensate for the unexpected behavior.

Table IX: Estimated resistance for test case 2

Link #	R(Ω)	Estimated R(Ω)	Link #	R(Ω)	Estimated R(Ω)	Link #	R(Ω)	Estimated R(Ω)
1	104	101.9	**18**	70	68.28	**35**	65.2	63.94
2	84.9	82.88	**19**	80.18	78.42	**36**	74.36	72.89
3	42.12	41.3	**20**	47.12	45.97	**37**	79.24	77.7
4	61.77	60.18	**21**	78.52	76.67	**38**	19.55	19.16
5	54.91	53.84	**22**	80.18	78.5	**39**	59.48	58.14
6	94.64	92.7	**23**	80.39	78.45	**40**	58.44	57.08
7	82.78	81.09	**24**	13.93	13.58	**41**	53.24	51.16
8	30.68	30.01	**25**	73.21	71.49	**42**	52.84	51.44
9	67.08	65.66	**26**	75.92	74.22	**43**	37.54	36.55
10	67.5	66.1	**27**	66.56	65.13	**44**	58.66	57.31
11	66.24	64.92	**28**	27.66	27.03	**45**	52.62	51.4
12	66.04	64.58	**29**	78.32	76.57	**46**	52.72	51.59
13	60.52	59.24	**30**	101.72	99.42	**47**	51.58	50.06
14	57	55.42	**31**	30.68	29.92	**48**	75.3	73.43
15	68.32	66.83	**32**	71.56	69.95	**49**	76.44	74.33
16	78.72	76.99	**33**	102.86	100.81	**50**	76.86	74.87
17	75.2	73.58	**34**	65.2	63.92			

5.5 Summary

In this chapter, an algorithm is described to identify the mismatch between the cable resistance in the model and the real system. The approach uses a quadratic programming technique to minimize the error between the power flow results and the observed values.

Chapter 6: Concluding Remarks

To effectively study the ocean, data needs to be collected by scientific instruments over an extended period of time. A cabled observatory system provides a suitable infrastructure for this purpose by providing power to these instruments. NEPTUNE is an underwater observatory located under the northeast Pacific Ocean that allows scientists to connect their instruments to the system. Power and communication capabilities are provided to users at the science nodes so that on-going studies of the processes under the ocean can be conducted. This dissertation deals with the design and implementation aspects of the NEPTUNE power system, including data monitoring and control, operations, and software modules development.

The design of the NEPTUNE power system involves a number of engineering challenges due to its physical location and the nature of a DC networked configuration: the development of an equivalent to the SCADA system and EMS of terrestrial power systems, the requirement of high reliability, lack of available measurements on the backbone to locate a fault within a small distance, insufficient power to supply all the loads, and changes in the resistance parameter that requires the ability to update system model. Solutions to meet these challenges are proposed in this dissertation. The contributions are summarized as follows:

1) The Power Monitoring and Control System (PMACS) is developed to provide the functions of SCADA and EMS for the NEPTUNE power system. PMACS consists of hardware and software modules for data handling, control operations, and system analysis. PMACS for the MARS test bed is implemented and has passed the factory acceptance test.
2) The Fault Location module of PMACS is developed to locate a backbone cable fault within ±1 km using only available measurements from the shore station and the system topology by solving simultaneous non-linear equations. The algorithm is a generalized version of the resistance

estimation technique used by point-to-point system. The generalization allows the algorithm to be used on networked systems. The same technique can be applied to underground power cables.

3) The Load Management module of PMACS is developed to determine the optimal load condition of the system based on non-linear optimization with the priorities of the science node loads. The objective is to maximize the total power delivered to the users while satisfying the system constraints.

4) A cable resistance identification algorithm is developed to update the parameters in the system model based on quadratic programming by comparing the power injections at the science nodes. The approach finds the optimal solution of the cable resistances based on the power flow output. The ocean temperature variation is taken into account.

The algorithms proposed in this dissertation provide solutions that address challenges and difficulties for an underwater observatory system. Similar systems would find the results presented in this dissertation to be applicable. Some algorithms developed such as the Fault Location module can be applied to underground power cables since the reliability requirement of such systems is similar to an underwater power system.

Bibliography

[1] *Maritime Communication Services.* [Online]. Available: http://www.mcs.harris.com/oceannet/oceannet.html.

[2] *Advanced Real-time Earth monitoring Network in the Area (ARENA).* [Online]. Available: http://homepage.mac.com/ieee_oes_japan/ARENA/ARENA-E.html.

[3] *European Sea Floor Observatory Network (ESONET)*. [Online]. Available: http://www.oceanlab.abdn.ac.uk/research/esonet.php.

[4] J. Kojima, K. Asakawa, B. Howe, H. Kirkham, "*Power Systems for Ocean Regional Cabled Observatories*," *Proc. Oceans 2004.* MTS/IEEE TECHNO-OCEAN '04*,* IEEE Oceans Conference, Vol. 4, 2004, pp.2176-2181.

[5] J. Delaney, G.R. Heath, A. Chave, H. Kirkham, B. Howe, W. Wilcock, P. Beauchamp, and A. Maffei, "NEPTUNE Real-Time, Long-Term Ocean and Earth Studies at the Scale of a Tectonic Plate," *Proc. Oceans 2001*, MTS/IEEE Conference and Exhibition, Vol. 3, 2001, pp. 1366-1373.

[6] B. Howe, H. Kirkham, and V. Vorperian, "Power System Considerations for Undersea Observatories," *IEEE J. Oceans Eng*., Vol. 27, No. 2, April 2002, pp. 267-274.

[7] B. Howe, H. Kirkham, V. Vorperian, and P. Bowerman, "The Design of the NEPTUNE Power System," *Proc. Oceans 2001*, MTS/IEEE Conference and Exhibition, Vol. 3, 2001, pp. 1374-1380.

[8] K. Schneider, C.C. Liu, T. McGinnis, B. Howe, and H. Kirkham, "Real-Time Control and Protection of the NEPTUNE Power System," *Proc. Oceans 2002*, MTS/IEEE Conference and Exhibition, Vol. 2, 2002, pp. 1799-1805.

[9] P. Fairley, "Neptune Rising," *IEEE Spectrum*, Vol. 42, No. 11, Nov. 2005, pp. 38-45.

[10] *North East Pacific Time-integrated Undersea Networked Experiments (NEPTUNE)*. [Online]. Available: http://www.neptune.washington.edu.

[11] M.A. El-Sharkawi, A. Upadhye, S. Lu, H. Kirkham, B. Howe, T. McGinnis, and P. Lancaster, "North East Pacific Time-Integrated Undersea Networked Experiments (NEPTUNE): Cable Switching and Protection," *IEEE J. Oceanic Eng.*, Vol. 30, No. 1, Jan. 2005, pp. 232-220.

[12] S. Lu, "Infrastructure, Operations, and Circuits Design of an Undersea Power System," *PhD Dissertation*, Electrical Engineering, University of Washington, , 2006, pp. 1-157.

[13] *Ocean research Interactive Observatory Networks (ORION) Report of Design and Implementation Workshop*. [Online]. Available: http://www.orionprogram.org/PDFs/DI_report_final.pdf.

[14] P. Phibbs and S. Lentz, "Selection of the Technical Design of the World's First Regional Cabled Observatory - NEPTUNE Stage 1 (NEPTUNE Canada)," *Proc. The Scientific Submarine Cable 2006 Conference*, Marine Institute, Dublin Castle, Dublin, Ireland, Feb. 2006.

[15] J.W. Evans, "Energy Management System Survey of Architecture," *IEEE Computer Applications in Power*, Vol. 2, No. 1, Jan. 1989, pp. 11 - 16.

[16] F.F. Wu, K. Moslehi, and A. Bose, "Power System Control Centers: Past, Present, and Future," *Proc. IEEE*, Vol. 93, No. 11, Nov. 2005, pp. 1890-1908.

[17] *IEEE Standard Definition, Specification, and Analysis of Systems Used for Supervisory Control, Data Acquisition, and Automatic Control*, IEEE Standard C31.1-1987, 1987.

[18] K. Schneider, "Analysis of Critical Infrastructure Interactions," *PhD Dissertation*, Electrical Engineering, University of Washington, 2005, pp. 1-174.

[19] M. Kezunovic, P. Spasojevic, C.W. Fromen, and D.R. Sevcik, "An Expert System for Transmission Substation Event Analysis," *IEEE Trans. Power Delivery*, Vol. 8, No. 4, Oct. 1993, pp. 1942-1949.

[20] J.A. Jiang, J.Z. Yang, Y.H. Lin, C.W. Liu, and J.C. Ma, "An Adaptive PMU Based Fault Detection/Location Technique for Transmission Lines. Part I: Theory and Algorithms," *IEEE Trans. Power Delivery*, Vol. 15, No. 2, April 2000, pp. 486-493.

[21] P. Menconi and D.J. Liparoto, "Tracking and Fault Location in Undersea Cables," *Proc. Oceans 1992*, Mastering the Oceans Through Technology, Vol. 2, 1992, pp. 678-683.

[22] P. Jazayeri, A. Schellenberg, W.B. Rosehart, J. Doudna, S. Widergren, D. Lawrence, J. Mickey, and S. Jones, "A Survey of Load Control Programs for Price and System Stability," *IEEE Trans. Power Systems*, Vol. 20, No. 3, Aug. 2005, pp. 1504-1509.

[23] C.F. Henville, "Digital Relay Reports Verify Power System Models," *IEEE Trans. Power Delivery*, Vol. 13, No. 2, April 1998, pp. 386-393.

[24] H. Kim, A. Abur, "Enhancement of External System Modeling for State Estimation," *IEEE Trans. Power Systems*, Vol. 11, No. 3, Aug. 1996, pp. 1380-1386.

[25] D.N. Kosterev, C.W. Taylor, and W.A. Mittelstadt, "Model Validation for the August 10, 1996 WSCC System Outage," *IEEE Trans. Power Systems*, Vol. 14, No. 3, Aug. 1999, pp. 967–979.

[26] R.H. Craven, T. George, G.B. Price, P.O. Wright, and I.A. Hiskens, "Validation of Dynamic Modeling Methods against Power System Response to Small and Large Disturbances," *Proc. CIGRÉ General Session*, Paris, Aug. 1994.

[27] I.A. Hiskens, "Nonlinear Dynamic Model Evaluation from Disturbance Measurements," *IEEE Trans. Power Systems*, Vol. 16, No. 4, Nov. 2001, pp. 702-710.

[28] D. Shi, X, Xie, and L. Tong, "Studies on Parameter Identification Using Genetic Algorithm in Power System," *Proc. Transmission and Distribution Conference and Exhibition: Asia and Pacific 2005*, Aug. 2005, pp. 1-5.

[29] B. M. Howe, T. Chan, M. El Sharkawi, M. Kenney, S. Kolve, C.C. Liu, S. Lu, T. McGinnis, K. Schneider, C. Siani, H. Kirkham, V. Vorperian, and P. Lancaster, "Power System for the MARS Ocean Cabled Observatory," *Proc. the Scientific Submarine Cable 2006 Conference*, Marine Institute, Dublin Castle, Dublin, Ireland, Feb. 2006.

[30] T. Baldwin, F. Renovich Jr., L.F. Saunders, and D. Lubkeman, "Fault Locating in Ungrounded and High-Resistance Grounded Systems," *IEEE Trans. Industry Applications*, Vol. 37, No. 4, July-Aug. 2001, pp. 1152-1159.

[31] J. Jung, C.C. Liu, M. Hong, M. Gallanti, and G. Tornielli, "Multiple Hypotheses and their Credibility in On-Line Fault Diagnosis," *IEEE Trans. Power Delivery*, Vol. 16, No. 2, April 2001, pp. 225-230.

[32] S. Navaneethan, J.J. Soraghan, W.H. Siew, F. McPherson, and P.F. Gale, "Automatic Fault Location for Underground Low Voltage Distribution Networks," *IEEE Trans. Power Delivery*, Vol. 16, No. 2, April 2001, pp. 346-351.

[33] P. Pilgrim, "Analysis and Location of Shunt Faults," 360networks, Internal Report, March 2000.

[34] *Electric Power Research Institute*, Palo Alto, CA. Project Set 128B, P128.002. [Online]. Available: http://www.epri.com/portfolio/product.aspx?id=1490&area=38&type=10.

[35] G.C. Lampley, "Fault Detection and Location on Electrical Distribution System Case Study," *Proc. Rural Electrical Power Conference*, May 2002, pp. B1-B1-5.

[36] K. Zimmerman and D. Costello, "Impedance-Based Fault Location Experience," *Proc. 58th Annual Conference for Protective Relay Engineers*, April 2005, pp. 211-226.

[37] K. Schneider, C.C. Liu, B. Howe, and H. Kirkham, "State Estimation for the NEPTUNE Power System," *Proc. Transmission and Distribution Conference*, Vol. 2, Sept. 2003, pp. 748-754.

[38] K. Schneider, C.C. Liu, and B. Howe, "Topology Error Identification for the NEPTUNE Power System," *IEEE Trans. Power Systems*, Vol. 20, No. 3, Aug. 2005, pp. 1224-1232.

[39] K.-H. Ng and G.B. Sheble, "Direct Load Control – A Profit-Based Load Management Using Linear Programming," *IEEE Trans. Power Systems*, Vol. 13, No. 2, May 1998, pp. 688-694.

[40] L. Effler, G. Schellstede, and H. Wagner, "Optimization of Energy Procurement and Load Management," *IEEE Trans. Power Systems*, Vol. 7, No. 1, Feb. 1992, pp. 327-333.

[41] Z.J. Paracha and P. Doulai, "Load Management: Techniques and Methods in Electric Power System," *Proc. Energy Management and Power Delivery*, Vol. 1, March 1998, pp. 213-217.

[42] R.G. Parker and R.L. Rardin, *Discrete Optimization*, Academic Press, San Diego, 1988, pp. 159-164.

[43] *The Ocean Bottom Properties Database*. [Online]. Available: http://www.iphc.washington.edu/Staff/hare/html/papers/OBT/obt.html.

[44] *Northeast Pacific Long Term Observation Program*. [Online]. Available: http://ltop.coas.oregonstate.edu/~ctd/index.html.

Vita

Ting Chan was born in Shanghai, China and grew up in Hong Kong. After graduating from high school in 1994, he came to the U.S. to attend university. He received his Bachelor of Science degree and Master of Science degree both from the University of Washington in 1999 and 2001 respectively. He is currently enrolled in the Ph.D. program in the Department of Electrical Engineering at the University of Washington. With the presentation and successful defense of this dissertation, he will have completed his Ph.D. in Electrical Engineering under Professor Chen-Ching Liu.

List of Publications

[1] T. Chan, C.C. Liu, and B.M. Howe, "Optimization Based Load Management for the NEPTUNE Power System," Accepted by *IEEE Power Engineering Society General Meeting 2007*, June 2007.

[2] T. Chan, C.C. Liu, B.M. Howe, and H. Kirkham, "Fault Location for the NEPTUNE Power System," *IEEE Trans. Power Systems*, Vol. 22, No. 2, May 2006, pp. 522-531.

[3] B.M. Howe, T. Chan, M. El Sharkawi, M. Kenney, S. Kolve, C.C. Liu, S. Lu, T. McGinnis, K. Schneider, C. Siani, H. Kirkham, V. Vorperian, and P. Lancaster, "Power System for the MARS Ocean Cabled Observatory," *Proc. the Scientific Submarine Cable 2006 Conference*, Marine Institute, Dublin Castle, Dublin, Ireland, Feb. 2006.

[4] T. Chan, C.C. Liu, and J.W. Choe, "Implementation of Reliability-Centered Maintenance for Circuit Breakers," *Proc. IEEE Power Engineering Society General Meeting 2005*, Vol. 1, June 2005, pp. 684-690.

[5] T. Chan, C.C. Liu, D. Lucarella, M. Gallanti, D. Sobajic, and M. Hofmann, "Intelligent Alarm Analysis: Generalization and Enhancement," *International Journal of Engineering Intelligent Systems*, Vol. 13, No. 2, June 2005, pp. 127-134.

[6] T. Chan, C.C. Liu, D. Lucarella, M. Gallanti, D. Sobajic, and M. Hofmann, "Intelligent Alarm Analysis: Generalization and Enhancement," Presented at 12th Intelligent Systems Application to Power System Conference, Lemnos, Greece, 2003.